Deciphering the potential niche of novel black yeast fungal isolates in a biological soil crust based on genomes, phenotyping, and melanin regulation

Erin C. Carr[1], Quin Barton[2], Sarah Grambo[3], Mitchell Sullivan[1], Cecile M. Renfro[4], Alan Kuo[5], Jasmyn Pangilinan[5], Anna Lipzen[5], Keykhosrow Keymanesh[5], Emily Savage[5], Kerrie Barry[5], Igor V. Grigoriev[5,6], Wayne R. Riekhof[1], Steven D. Harris[7,8]*

1) University of Nebraska-Lincoln, School of Biological Sciences, Lincoln, Nebraska 68588; 2) University of Nebraska-Lincoln, Department of Biochemistry, Lincoln, Nebraska 68588; 3) Iowa State University, Roy J. Carver Department of Biochemistry, Biophysics, and Molecular Biology, Ames, Iowa 50011; 4) University of Nebraska-Lincoln, Department of Agronomy and Horticulture, Lincoln, Nebraska 68588; 5) US Department of Energy Joint Genome Institute Lawrence Berkley National Laboratory, Berkley California 94720; 6) Department of Plant and Microbial Biology, University of California Berkeley, Berkeley, California 94720; 7) Iowa State University, Department of Plant Pathology and Microbiology, Ames, Iowa 50011; 8) Iowa State University, Department of Entomology Ames, Iowa 50011

Abstract

Black yeasts are polyextremotolerant fungi that contain high amounts of melanin in their cell wall and maintain a primarily yeast form. These fungi grow in xeric, nutrient deplete environments which implies that they require highly flexible metabolisms and the ability to form lichen-like mutualisms with nearby algae and bacteria. However, the exact ecological niche and interactions between these fungi and their surrounding community is not well understood. We have isolated two novel black yeast fungi of the genus *Exophiala*: JF 03-3F "Goopy" *E. viscosium* and JF 03-4F "Slimy" *E. limosus*, which are from dryland biological soil crusts. A combination of whole genome sequencing and various phenotyping experiments have been performed on these isolates to determine their fundamental niches within the biological soil crust consortium. Our results reveal that these *Exophiala* spp. are capable of utilizing a wide variety of carbon and nitrogen sources potentially from symbiotic microbes, they can withstand many abiotic stresses, and can potentially provide UV resistance to the crust community in the form of secreted melanin. Besides the identification of two novel species within the genus *Exophiala*, our study also provides new insight into the production and regulation of melanin in extremotolerant fungi.

Background

Polyextremotolerant fungi are a polyphyletic group of fungi that can be broken down into black yeast fungi and microcolonial fungi. These two sub-types are distinct in their morphology; black yeast fungi are usually only yeasts but can be dimorphic, whereas microcolonial fungi are typically filamentous, pseudohyphal, or possess other unique morphologies such as spherical cells (Ametrano et al., 2017; De Hoog et al., 2003; Gostinčar et al., 2011). However, all polyextremotolerant fungi share the capacity to produce melanin, which presumably accounts for much of their polyextremotolerance. Most polyextremotolerant fungi are in the subdivision Pezizomycotina, residing mainly within Eurotiomycetes and Dothidiomycetes, but one could argue that any fully melanized fungus could be a polyextremotolerant fungi (Gostinčar et al., 2009).

Melanin is arguably a defining feature of polyextremotolerant fungi given that the form black colonies that are easily distinguishable from those formed by non-melanized fungi. Because of its association with the cell wall, melanin imbues polyextremotolerant fungi with resistance to multiple forms of stress.

Most commonly known is UV-resistance as melanin absorbs light in the UV part of the spectrum, but melanin is also capable of absorbing ROS, RNS, metals, reducing desiccation, and potentially using ionizing radiation as an energy source (Cordero & Casadevall, 2017; Dadachova et al., 2007). Collectively, these features of melanin are thought to enhance the ability of polyextremotolerant fungi to colonize habitats that are otherwise inhospitable to most forms of life.

The production of melanin is a key functional trait observed in fungi spanning the fungal kingdom (Bell & Wheeler, 1986; Zanne et al., 2020). The diverse protective functions of melanin (e.g., metal resistance, ROS and RNS tolerance, UV resistance) (Cordero & Casadevall, 2017; Gessler et al., 2014; Płonka & Grabacka, 2006; Zanne et al., 2020) underscores its broad utility in mitigating the impacts of stress despite the potential cost of its synthesis (Schroeder et al., 2020). Fungi are capable of producing three different types of melanin: pheomelanin, allomelanin, and pyomelanin, all of which have their own independent biosynthetic pathways. Allomelanin, is formed from the polymerization of 1,8-DHN, which requires the use of polyketide synthase for initial steps in production (Perez-Cuesta et al., 2020; Płonka & Grabacka, 2006) (**Figure 1**). Pyomelanin and pheomelanin share an initial substrate of Tyrosine, but pheomelanin derives from L-DOPA, whereas pyomelanin is created via tyrosine degradation (Perez-Cuesta et al., 2020; Płonka & Grabacka, 2006) (**Figure 1**). Allomelanin and pheomelanin are often referred to as DHN melanin and DOPA melanin respectively, given their chemical precursors. Unfortunately, due to the unique characteristics of melanins and their association with larger biomolecules, we do not know the complete structure of any type of melanin (Cao et al., 2021). However, given that we do know their chemical constituents, it is possible to draw some inferences about the relationship between structure and function of a particular type of melanin. For instance, out of the three types of melanin fungi can produce only pheomelanin has a chemical precursor, 5-CysDOPA, with both Nitrogen and Sulfur in its structure (Płonka & Grabacka, 2006). Notably, all three fungal melanins are synthesized via independent pathways, which enables the targeted use of chemical inhibitors to block one pathway without interfering with the others. For example, previous studies have extensively used the chemical melanin blockers kojic acid and phthalide to block pheomelanin and allomelanin respectively (Pal et al., 2014) (**Figure 1**). Use of these chemical blockers allowed previous studies to identify the primary melanin biosynthetic pathway employed by individual fungal species (Pal et al., 2014).

Polyextremotolerant fungi tend to occupy extreme niches such as rock surfaces, external brick and marble walls, soil surfaces, and even the inside of dishwashers (Gostinčar et al., 2009; Zupančič et al., 2016). Characteristic features of these environments includes the relative paucity of nutrients and the frequent presence of a community biofilm consisting of photosynthetic organisms and/or bacteria (Gostinčar et al., 2012). Strikingly, these species are rarely found alone in their habitats, which suggests that multi-species interactions between fungi, bacteria, and photosynthetic organism underlie the formation and function of these communities. That is, the ability of polyextremotolerant fungi to successfully adapt to their niche must depend on complex yet poorly understood interactions with other microbes..

We have isolated two polyextremotolerant fungi from a biological soil crust (BSC) at Jackman Flats Provincial Park in B.C., Canada. These novel fungi are of the genus *Exophiala*, this genus has previously been found in BSCs (Bates et al., 2006). Biological soil crusts are unique dryland biofilms that form on the surface of xeric desert soils where little to no plants are able to grow (Belnap, 2003; Belnap et al., 2001). They are notable for their extensive cyanobacteria population, which seeds the initial formation

of all biological soil crusts and creates the main source of nitrogen for the rest of the community (Belnap, 2002). Once the initial crust is established, it is then inundated with a consortium of bacteria, fungi, algae, archaea, lichens, and mosses (Bates et al., 2010; Lan et al., 2012; Maier et al., 2016). This community is a permanent fixture on the land they occupy unless physically disturbed, much like other biofilms (Belnap & Eldridge, 2001; Donlan & Costerton, 2002).

As a result of the desert conditions biological soil crusts reside in, the microbes found there are constantly exposed to extreme abiotic factors which they must tolerate simultaneously (Bowker et al., 2010). Some of these abiotic extremes are: UV radiation (especially at higher altitudes and closer to the poles) (Bowker et al., 2002), desiccation and osmotic pressures (Rajeev et al., 2013), and temperature fluctuations both daily and annually (Belnap et al., 2001; Bowker et al., 2002; Pócs, 2009). Microbes that reside in these biological soil crusts have therefore adapted mechanisms to withstand these abiotic extremes.

Extensive amount of research has been dedicated to certain members of the biological soil crust community, but one such less studied microbe has been the “free-living” fungal taxa. These fungi are non-lichenized yet are still thriving in an environment where there are no plants to infect or decompose, and no obvious source of nutrients besides contributions from the other members of the biological soil crust community. This would imply that even though these fungi are not lichenized per say, they would have to be engaging in lichen-like interactions with the biological soil crust community to obtain vital nutrients for proliferation. While the idea of transient interactions between non-lichenized fungi and other microbes has been floated by previous researchers in other systems (Gostinčar et al., 2012; Grube et al., 2015; Hom & Murray, 2014), it will be a difficult task to strongly confirm in biological soil crusts given their taxonomic complexity.

Biological soil crusts (BSCs) are a multi-kingdom biofilm on the surface of arid soils that exhibit little or no plant growth (Belnap et al., 2001). Despite the importance of microbial interactions in enabling the successful formation of BSCs in a niche characterized by poor nutrient and water availability, the fungal components of BSCs and their relative functions within the interaction network remain poorly understood. Here, we combine genome sequencing with computational tools and culture-based phenotyping to isolate and describe two new species of black yeast fungi associated with BSCs. We report on their carbon and nitrogen utilization profiles, stress responses, and lipid accumulation patterns. In addition, we characterize their capacity for melanin production and generate valuable insight into mechanisms that might be involved in regulating the synthesis of these compounds.

Methods

Fungal Strains and Media

Two novel species of fungi are described here: *Exophiala viscosium* and *Exophiala limosus*. Their genomes are deposited at DOE JGI in Mycocosm (*E. viscosium*: https://mycocosm.jgi.doe.gov/EurotioJF033F_1/EurotioJF033F_1.home.html; *E. limosus*: https://mycocosm.jgi.doe.gov/EurotioJF034F_1/EurotioJF034F_1.home.html). Their type strains have been deposited to the Westerdijk institute. *E. viscosium* and *E. limosus* are typically grown in malt extract medium (MEA; see **Table 1** for media recipe) at room temperature in an Erlenmeyer flask at 1/10th the volume of the flask, shaking at 200 rpm. Additional strains used were *Saccharomyces cerevisiae* ML440 and BY4741, and *E. dermatitidis* WT strain ATCC 34100. *S. cerevisiae* strains are grown

in Yeast Peptone Dextrose medium (YPD; see **Table 1** for media recipe), and *E. dermatitidis* is grown in MEA.

Fungal isolation and identification methods

Fungi were isolated from public land in B.C., Canada. Soil samples were taken from the top 2 cm of biological soil crusts. A 0.1 g portion was re-suspended in water, ground with a sterile micropestle, and diluted with a DF of 10 till they reached 10,000x dilution. Each dilution was then spread out onto two different MEA petri plate containing either no antibiotics or containing: Ampicillin (100 mg/L), Chloramphenicol (50 mg/L), Gentamycin (10 mg/L), and Cycloheximide (400 mg/L). The plates were then incubated in a Percival light incubator at 23° C with a 12 hr light/dark cycle and examined daily using a dissection microscope to check for small black colonies. Once a potential black colony was seen, half of it was removed and transferred to a new MEA (no antibiotics) petri plate. It was vital to examine the plates daily, because even in the presence of antibiotics many unwanted fast-growing microbes would grow on the plates and cover up the slower growing polyextremotolerant fungal colonies. Once a pure culture of each isolate was grown up (approximately 2 weeks), they were preserved in 30% Glycerol and stored in the -80° C freezer. DNA sequencing of amplified ITS sequences was used to identify the isolates. DNA was extracted using the Qiagen DNeasy Powersoil DNA extraction kit. Primers used to isolate the ITS region were: ITS1- (5'-TCC GTA GGT GAA CCT GCG G-3') and ITS4- (5'-TCC TCC GCT TAT TGA TAT GC-3') (White et al., 1990). A BioRad MJ Mini Personal Thermal Cycler was used, with the program set as: 1) 95° C for 5:00 (5 minutes), 2) 94° C for 0:30 (30 seconds), 3) 55° C for 0:30, 4) 72° C for 1:30, 5) Return to 2 35 times, 6) 72° C for 5:00. Resulting PCRs were then checked via gel electrophoresis in 1% agar run at 80 V for 1 hr. Isolated ITS regions were sequenced using the Eurofins sequencing facility, and the sequences were subsequently BLASTed against the NCBI database to look for potential matches.

DNA extraction and RNA extraction for whole genome sequencing

A CTAB-based DNA extraction method was performed to obtain high molecular weight DNA for whole genome sequencing. The DNA extraction method used was derived from (Cubero et al., 1999). Changes to the original protocol include: switching PVPP for the same concentration of PVP, use of bead beating tubes with liquid nitrogen-frozen cells and the extraction buffer instead of a mortar and pestle for breaking open the cells, and heating up the elution buffer to 65° C before eluting the final DNA. These changes were made to optimize the protocol for liquid-grown yeast cells instead of lichen material. Cells for the DNA extraction were grown up in 25 mL of liquid MEA in 250 mL Erlenmeyer flasks for 5 days, 1 mL of those grown cells was used for the DNA extraction after washing with water.

RNA was obtained using the Qiagen RNeasy mini kit (Cat. No. 74104). Cells were grown in 25 mL of three different liquid media types (MEA, YPD, and MNV) in 250 mL Erlenmeyer flasks at room temperature for 5 days, and 1-2 mL of cells were used for the RNA extraction. Cells were washed with DEPC-treated water and flash frozen in liquid nitrogen in 1.5 mL microcentrifuge tubes. RNA extraction was then performed according to the methods by the RNeasy kit.

Genome assembly and annotation

Both genomes and transcriptomes were sequenced using Illumina technology. For transcriptomes, a plate-based RNA sample prep was performed on the PerkinElmer Sciclone NGS robotic liquid handling

system using Illuminas TruSeq Stranded mRNA HT sample prep kit utilizing poly-A selection of mRNA following the protocol outlined by Illumina in their user guide: https://support.illumina.com/sequencing/sequencing_kits/truseq-stranded-mrna.html, and with the following conditions: total RNA starting material was 1 ug per sample and 8 cycles of PCR was used for library amplification. The prepared libraries were quantified using KAPA Biosystems' next-generation sequencing library qPCR kit and run on a Roche LightCycler 480 real-time PCR instrument. The libraries were then multiplexed and prepared for sequencing on the Illumina NovaSeq sequencer using NovaSeq XP v1 reagent kits, S4 flow cell, following a 2x150 indexed run recipe.

Using BBDuk (https://sourceforge.net/projects/bbmap/), raw reads were evaluated for artifact sequence by kmer matching (kmer=25), allowing 1 mismatch and detected artifact was trimmed from the 3' end of the reads. RNA spike-in reads, PhiX reads and reads containing any Ns were removed. Quality trimming was performed using the phred trimming method set at Q6. Finally, following trimming, reads under the length threshold were removed (minimum length 25 bases or 1/3 of the original read length - whichever is longer). Filtered reads were assembled into consensus sequences using Trinity ver. 2.3.2 (Grabherr et al., 2011).

For genomes, DNA library preparation for Illumina sequencing was performed on the PerkinElmer Sciclone NGS robotic liquid handling system using Kapa Biosystems library preparation kit. 200 ng of sample DNA was sheared to 300 bp using a Covaris LE220 focused-ultrasonicator. The sheared DNA fragments were size selected by double-SPRI and then the selected fragments were end-repaired, A-tailed, and ligated with Illumina compatible sequencing adaptors from IDT containing a unique molecular index barcode for each sample library. The prepared libraries were quantified using KAPA Biosystems' next-generation sequencing library qPCR kit and run on a Roche LightCycler 480 real-time PCR instrument. The quantified libraries were then multiplexed with other libraries, and the pool of libraries was then prepared for sequencing on the Illumina HiSeq sequencing platform utilizing a TruSeq paired-end cluster kit, v4, and Illumina's cBot instrument to generate a clustered flow cell for sequencing. Sequencing of the flow cell was performed on the Illumina HiSeq2500 sequencer using HiSeq TruSeq SBS sequencing kits, v4, following a 2x150 indexed run recipe.

An initial assembly of the target genome was generated using VelvetOptimiser version 2.1.7 (3) with Velvet version 1.2.07 (Zerbino & Birney, 2008) using the following parameters; "--s 61 --e 97 --i 4 --t 4, --o "-ins_length 250 -min_contig_lgth 500"". The resulting assembly was used to simulate 28X of a 2x100 bp 3000 +/- 300bp insert long mate-pair library with wgsim version 0.3.1-r13 (https://github.com/lh3/wgsim) using "-e 0 -1 100 -2 100 -r 0 -R 0 -X 0 -d 3000 -s 30". 25X of the simulated long mate-pair was then co-assembled together with 125X of the original Illumina filtered fastq with AllPathsLG release version R49403 (Gnerre et al., 2011) to produce the final nuclear assembly. The genome was annotated using JGI Annotation pipeline (Grigoriev et al., 2013). The assemblies and annotations of bot genomes are available at the fungal genome portal MycoCosm ((Grigoriev et al., 2014); https://mycocosm.jgi.doe.gov) and in the DDBJ/EMBL/GenBank repository under accessions XXXXXXX and XXXXXXXX.

Mating type locus identification

Mating loci for *E. viscosium* and *E. limosus* were determined using the methods described by Teixeira et al. (2017). Genes known to flank the MAT loci of most Chaetothyriales species include: *APN2*, *SLA2*, *APC5*, and *COX13*. The protein sequences of these genes from *Aspergillus nidulans* were used to BLASTP

against the genomes of the new fungi. These gene sequences were obtained from Aspergillus Genome Database and BLASTed using JGI's Mycocosm. Once those genes were found, analysis of upstream and downstream flanking genes was performed until the mating gene MAT1-1 was located. Genes close to MAT1-1 and within the span of genes listed above were considered part of the MAT locus.

Phenotyping experiments:

Budding Pattern determination

Protocols for observing the budding patterns of these new species were derived from methods in (Mitchison-Field et al., 2019). A 1:1:1 ratio of Vaseline, Parafin, and Lanolin (VALAP) was combined in a glass bottle and heated to 115° C to melt completely and kept at room temperature for later use. Heated solid MEA was aliquoted into a 50mL tube for agar slab making. Isolates were grown in liquid MEA for 5 days prior to inoculation of slides. First, the VALAP was brought back up to 115° C to melt completely for application. Then 5 µL of the 5-day old cells were diluted in 995 µL of liquid MEA. Agar slabs of MEA were made by microwaving the 50 mL tube of solid MEA until it melted, then pipetting 1 mL of the hot agar into a 1 cm x 2 cm mold formed out of cut strips of silicone and laid down in a sterile petri dish. This agar slab was allowed to solidify and was then cut in half to be 1 cm x 1 cm. Both the cover slip and the slide were wiped down with ethanol to ensure clean and sterile growth conditions for the cells. 8 µL of the diluted cells was pipetted onto the center of the sterile slide, then one square of the agar slab was carefully placed on top of the cells in media, 8uL of MEA was pipetted onto the top of the agar slab, and the coverslip was placed over the agar slab. Using a small paintbrush, the melted VALAP was carefully painted onto the gap between the coverslip and the microscope slide to seal off the coverslip. Finally, a 23-gauge needle was used to poke holes in the solidified VALAP to allow for gas exchange.

The slide was then placed with the slide facing down onto the inverted microscope EVOS fl. Once an adequate number of cells was observed in frame, the cells were allowed to settle for 2 hours before imaging began. Images were then automatically taken every 30 mins for 72 hours. Videos of the budding pattern were created using Adobe Premiere Pro.

Growth of E. viscosium and E. limosus on different medias

Eight different fungal media were used to observe the growth of these novel fungi. These media have been used for identification purposes and will be useful for future identification of these species from other locations. Media used in this experiment were: MAG, MEA, MN, MNV, MN+NAG, PDA, Spider, YPD, V8 (**Table 1**). Both isolates were first grown in 25 mL of liquid MEA at room temperature, shaking at 200 rpm for 5 days. Then 1 mL of each species was aliquoted and washed 3 times with water. Washed cells were then applied to the media in three ways: 5 µL spotting (pipetting 5 µL of cells onto the plate), toothpick poking (poking a sterile toothpick tip into the suspended cells and then onto a plate), and metal loop streaking (placing sterile metal loop into suspended cells, then spreading cells onto plate in a decreasing manner). This provided us with different plating techniques that could potentially yield different morphologies.

Carbon Utilization

Carbon utilization of each isolate was determined using a BioMerieux ID C32 carbon utilization strip (Cat. No. 32200-1004439110). These strips have 30 different carbon sources in individual wells, one well with

no carbon source for a negative control, and one well with Ferric citrate. The inoculated strips were kept in a plastic container with a lid and lined with moist paper towels to reduce drying. The initial inoculum of cells was prepared in 25 mL of MEA shaking at room temp for 5 days. Inoculation of the strips was done according to the instructions provided by the vendor, and each strain was inoculated in three separate strips for triplicate replication. Cells were diluted to the kit requirement of McFarland standard #3 before starting the inoculum. Growth in the ID strip lasted 10 days before evaluation. Growth in each well was observed and evaluated by eye. Each well was compared to the negative control (no carbon) and the positive control (dextrose). Initial growth was evaluated on a: +, V, -, and - - scale. If a well had the same growth as the negative control it was given a "-", meaning no growth; if the well had less growth than the negative control it was given a "- -", meaning growth was inhibited by the carbon source; if a well had growth equal to or more than the dextrose well then it was given "+", meaning it was capable of growth on the carbon substrate; finally if the well was in between the negative control and positive control it was given a "V", for variable growth. Nuances of the fungal growth on individual carbon sources required a more gradual scale, and so scores were adjusted to form a range of 1-5 to allow for more easy average calculation between the three replicates.

Nitrogen utilization

Nitrogen utilization tests were performed using ten different nitrogen conditions. 100 mM was the concentration used for all compounds that contained one nitrogen atom per molecule: Proline, Ammonium tartrate dibasic, Serine, Sodium Nitrate, Glycine, Glutamate, and Aspartate; 50 mM was the concentration used for Urea because it has two atoms of nitrogen per molecule; 1% w/v of Peptone was used as a positive control; and no nitrogen was added as a condition for a negative control (**Table 2**). Liquid minimal media (MN) with MN salts (not 20x Nitrate salts) was used with the varying nitrogen sources to ensure that no alternative nitrogen source would be available to the fungi. Fungi were first grown up in liquid MEA for 5 days at room temperature to reach maximum density. Then, 1 mL of cells was removed and washed three times with water. 99 µL of each medium was added to six wells in a 96-well plate, for six replicates, and 1 µL of the washed cells was added to each well. 100 µL of each medium was also added to one well each without cells to blank each condition, because the different nitrogen sources created different colors of medium. Daily growth was measured from day 0 to day 7 at 420 nm, using the BioTek Synergy H1 hybrid spectrophotometer.

Optimal growth temperature and range of growth temperatures

To determine the temperature resistance range and optimal growth temperature for each isolate, we grew them in 4° C, 15° C, Room temp at 23° C (i.e., ambient room temperature), 28° C, 37° C, and 42° C. Isolates were first grown up in 25 mL of MEA for 5 days at room temperature to maximum density. Then 1 mL of cells was removed, and a 10x serial dilution was made from 0x to 100,000x, using pre-filled 1.5mL tubes with 900 µL of MEA and adding 100 µL of the previous tubes each time. Then 5 µL of each serial dilution was spotted onto a square MEA plate which allowed us to determine the carrying capacity of each isolate at the different temperatures. Plates were kept at their respective temperatures for 7 days before observations were made, however the 37° C and 42° C incubators required cups of water inside of them to prevent the plates from dehydrating. Plates grown in 42° C and 37° C were then allowed to grow at room temp for up to a week to determine if the isolates died at these temperatures or if their growth was just arrested.

UV resistance

Resistance to UV light was observed to determine if these black fungi, with highly melanized cell walls and constant exposure to sunlight in their natural habitat, were in fact UV resistant. To determine this, we used the UVP HL-2000 HybriLinker UV crosslinker as our source of UV light. Individual isolates were inoculated in 25 mL of MEA and let grow under shaking conditions at 200 rpm for 5 days at room temperature to reach maximum density. 100 µL of this culture was then spread out onto 6 MEA plates, using a glass spreader. Three plates were kept as the control growth, to compare to the three other plates which were exposed to the UV light. Experimental plates were placed inside of the crosslinker with their lids taken off, lids kept inside the crosslinker, and both lids and petri dishes facing up. Then the plates were exposed to 120 seconds of UV light from a distance of 9.5 cm to the light source at 10,000 µJ/cm^2 (254 nm) (Frases et al., 2007). We then wrapped all plates in aluminum foil and placed them in the Percival light incubator set at 23°C for 2 days. After 2 days the plates were removed from the aluminum foil and left in the incubator for 5 more days before final observations. To determine whether a particular isolate was resistant to UV exposure, the growth of the isolate exposed to UV was compared to the control growth.

Metal Resistance

Metal resistance is a relatively universal trait in many polyextremotolerant fungal species. Due to the under-studied nature of this particular characteristic in biological soil crusts and fungi, we decided to test if any of our isolates were resistant to any heavy metals which would indicate possible bioremediation capacity. In order to test metal resistance, we used the antibiotic disc method by aliquoting metal solutions onto paper discs and observing zones of clearance. Metals and concentrations used are listed in **Table 3** For testing, 5 µL of each metal solution was aliquoted onto a dry autoclaved Wattman filter paper disc. These discs were then allowed to air dry and kept at 4° C for up to a week. Initial growth of the fungal isolates was done in 25 mL of MEA, shaking at 200 rpm for 5 days at room temperature. We then spread 100uL of each fungal isolate onto 100 mm sized MEA plates using a glass spreader to create a lawn. Using flame sterilized tongs our metal paper discs were placed onto the center of the petri dish on top of the fungal lawn and lightly pressed down to ensure the metal disc was touching the plate completely. These plates were then placed in the Percival light incubator at 23° C with a 12 hr light/dark cycle for up to 2 weeks. Once the plates were observed to have grown enough (1-2 weeks), the zone of clearing was measured in cm. Generally, large zones of clearing indicated sensitivity to the metal, whereas zones of reduced size were consisted with resistance to the metal.

Lipid profiles

Comparison of the lipid production of *S. cerevisiae*, *E. dermatitidis*, *E. viscosium*, and *E. limosus* was performed in the presence of fermentable vs. non-fermentable sugars in high and low nitrogen In order to test the lipid profile and growth changes associated with fermentable and non-fermentable sugars and differences in nitrogen source amounts we grew all four species in four different media types. 1) MEA; 2) MEA + 20 g/L of peptone instead of 2 g/L; 3) MEA with the dextrose replaced with the same weight amount of glycerol; 4) MEA with glycerol instead of dextrose and 20 g/L of peptone instead of 2 g/L. All four fungal species were first inoculated in 25 mL of liquid MEA in a 250 mL Erlenmeyer flask and shaken at 200 rpm for 5 days at room temperature to reach peak density. Then 100 µL was inoculated into 5 mL of each media in a size 25 mm tube, placed in a roller drum and allowed to grow at room temperature for 5 days. The inoculum of each fungus was aliquoted to ensure the same wet weight of each organism was present to compare lipid amounts across the four species.

To observe their lipid profile, we performed a standard lipid extraction. Cells were pelleted and re-suspended in 2 mL of methanol inside of glass tubes. Tube openings were covered in Durafilm before applying the lid of the tube, then samples were boiled for 5 minutes and let cool for 10 minutes. Then 2 mL of chloroform and 1.6 mL of 0.9% NaCl were added, and the tubes were vortexed to fully mix. Tubes were then centrifuged at 5000 rpm for 5 minutes to separate the layers. The bottom lipid layer of the suspension was removed and placed in a new glass tube which was then dehydrated using nitrogen gas till the samples became fully dry. Dehydrated samples were then re-suspended with 100 µL of a 9:1 ratio of chloroform : methanol to run the thin layer chromatography (TLC) with. For all samples except the *S. cerevisiae*, 7 µL of the lipid suspension was used to dot the TLC. For *S. cerevisiae,* 10 µL of the lipid suspension was needed. The solvent systems used for TLC were Chloroform : methanol : glacial acetic acid: water 85:12.5:12.5:3 for the Polar lipid solvent system, and Petroleum ether : Diethyl ether : acetic acid 80:20:1 for the neutral lipid solvent system. The TLC plates were loaded with 7 or 10 µL of the re-suspended samples, and they were placed in the Polar solvent system for approximately 30 minutes (half-way up the plate) before transferring to the Neutral Lipid solvent system in a separate container till the solvent front reached just a few cm below the top of the plate. The plate was then removed and dried for 15 minutes, until the solution on the plate was no longer volatile, and the plate was placed in the presence of iodine (Sigma-Aldrich cat. No. 207772) in a glass chamber for 5 minutes until all the lipids were visible. The plates were then immediately placed in plastic covers and scanned and photographed for visualization and documentation.

Melanin experiments:

Melanin biosynthesis gene annotation

Melanin biosynthesis in fungi occurs via three different pathways: the DHN pathway which creates allomelanin, the DOPA pathway which creates pheomelanin, and the tyrosine degradation pathway which creates pyomelanin (Cao et al., 2021; Gessler et al., 2014). Most fungal species only contain one melanin biosynthetic pathway, but there are many species in Pezizomycotina, particularly in the genera *Aspergillus* and *Exophiala*, which are capable of producing all three forms of melanin (Teixeira et al., 2017). For that reason, we decided to manually annotate the genes involved in all three melanin biosynthetic pathways in *E. viscosium* and *E. limosus* to determine if they too possessed all three melanin biosynthetic pathways. In all cases, the relevant *A. niger* genes were used as queries (Teixeira et al., 2017). Protein sequences for each gene were found using the Aspergillus genome database and were tested using BLAST-P against the filtered model proteins database of *E. viscosium and E. limosus* in Mycocosm (https://mycocosm.jgi.doe.gov/pages/blast-query.jsf?db=EurotioJF033F_1; https://mycocosm.jgi.doe.gov/pages/blast-query.jsf?db=EurotioJF034F_1. Since *A. niger* contains paralogs for some melanin biosynthetic genes, all genes listed in (Teixeira et al., 2017) were used as queries for BLAST searches. Once the melanin biosynthetic genes in *E. viscosium* and *E. limosus* were identified, their highest matching protein sequences were then reverse BLASTed to the *A. niger* genome to determine the reciprocal best hit and ensure true homology.

Regulation of Melanin production using chemical blockers

Once it was established that both isolates contain the potential for production of all three fungal melanins, the effects of known chemical blockers of the DHN and DOPA melanin pathways was used to investigate melanin production. DHN melanin blocker Phthalide and the DOPA melanin blocker Kojic

acid were both used in hopes of blocking melanin production in these isolates. Stock solutions were made according to (Pal et al., 2014): Phthalide was diluted in 70% ethanol, and Kojic acid in DMSO. Three separate experiments were performed using these melanin blockers, to determine which method would provide the most informative results.

The first was the disc diffusion method whereby Whatman filter paper discs were autoclaved and impregnated with 5 µL of either 10 mM of Phthalide or 10 mg/mL of Kojic acid. Impregnated filter paper discs were then placed on top of freshly spread lawns of either isolates on both MEA and YPD. Lawns were of 50:50 diluted 5-day old cells grown in MEA, and 100 µL of this dilution was spread onto the petri plates with a glass hockey stick. These plates were then grown at 23° C with 12 hr light/dark cycles for 5 days. Additionally, both a Kojic acid disc and Phthalid discs were placed on fungal lawns ~4 cm apart simultaneously to observe their specific melanin-blocking capabilities on the same cells.

Next, we tried adding the melanin blockers directly to the medium as was done in (Pal et al., 2014). Since melanin is more universally distributed in *Exophiala* cells compared to *Aspergillus* cells, we decided to use the highest concentration of both Kojic acid and Phthalide that was used by (Pal et al., 2014), which was 100 mM of each compound. This concentration was added to both solid YPD and MEA after autoclaving, individually and combined. These plates were then used for two forms of growth experiments. Alternatively, we spread a lawn onto YPD and MEA with and without Kojic acid, Phthalide, and both compounds at 100 mM each. Finally, we performed a 10x serial dilution of both *E. viscosium* and *E. limosus* up to 10,000x diluted, and spotted 5 µL of each dilution onto MEA plates with and without Kojic acid, Phthalide, and both compounds. We let both growth experiments grow at 23° C for 5 days with a 12 hr light/dark cycle.

Melanin Extraction and spectrophotometric measurements

Extraction of melanin from a variety of sources has been performed with two main categories of methods: chemical extraction and enzymatic extraction (Pralea et al., 2019). We were unsure which extraction method would be most applicable to these species, so both were performed. The enzymatic extraction method that was used came from (Rosas et al.) (2000). Alternatively, the chemical extraction method, which has been used more extensively in previous work, was derived from (Pal et al., 2014). Adjustments to the Pal et al. method included the initial precipitation of melanins in HCl took multiple days instead of overnight, and stopping the protocol when 2M NaOH was added to the extracted melanin. We did not continue on to re-precipitation and drying of the melanin as this product did not reprecipitate in any solvents used.

Exact methods are as follows. 10 mL of filter sterilized supernatant was transferred into a 50 mL centrifuge tube, and 40 mL of 6M HCl was added to the tube. The filtrate was then allowed to precipitate out for up to two weeks. Precipitated tubes were then centrifuged at 4000 rpm for 3 minutes, and the resulting supernatant was discarded. The pellet was washed with 2 mL of dd H2O, vortexed, centrifuged, and the supernatant discarded. Then 3 mL of 1:1:1 Chloroform : ethyl acetate : ethanol was added to the samples and vortexed vigorously to ensure as much re-distribution of the melanin was accomplished. The tubes were then centrifuged again, and any resulting clear layers (top and or bottom) were discarded, leaving behind the dark layer. 2 mL of water was added to the sample for washing, and the tubes were centrifuged again, and the entire supernatant was discarded. Finally, 1 mL of 2M NaOH was added to each sample to allow for a standard volume added even if the melanin amount and therefore the final volume varied.

Samples suspended in 1 mL of 2M NaOH were then diluted 5 µL into 195 µL of 2M NaOH into a 96-well plate, with a 200 µL 2M NaOH blank well. These diluted samples were then read using the BioTek Synergy H1 hybrid spectrophotometer. The settings were for a full spectrum read from 230 nm to 700 nm. However, the machine could not read ODs above 4.0, and therefore only data from 300 nm to 700 nm was used.

Melanin secretion and its concentration in the supernatant

To confirm that *E. viscosium* and *E. limosus* are actively secreting melanin, as opposed to dead cells lysing and releasing it, we grew both species and took daily aliquots for melanin extraction. Additionally, we wanted to compare the melanin secretion capabilities of these species to *E. dermatitidis* for a baseline comparison. All three species were grown up in liquid MEA shaking at room temperature for 5 days. Then 2 mL of cells were washed with water three times. 500 µL of washed cells were then inoculated into 100 mL of MEA and YPD in 500 mL flasks. We let the cells grow at 23° C shaking at 200 rpm for 7 days, removing 11 mL of cells and supernatant daily and pipetting them into 15 mL centrifuge tubes. The tubes of cells were then centrifuged at 3000 rpm for 5 minutes, the supernatant was removed, filter sterilized through a 0.2 µm filter, and placed into a new tube. We filter sterilized the supernatant to ensure that no cells remained in the supernatant, therefore all of the melanin extracted came only from secreted melanin. Melanin was then extracted using the chemical method explained above. Resulting pure melanin for all samples was read with the full spectrum as stated above, and both standard OD and log scale graph were created to confirm the existence of melanin.

Increasing amounts of peptone

To assess the role of nitrogen levels in melanin secretion, we initially switched the concentration of peptone added to YPD and MEA media; the new media would be: YPD + 0.2% peptone, and MEA + 2% peptone. We then took both *E. viscosium* and *E. limosus* that was grown in liquid MEA for 5 days shaking at room temperature, and plated out the species onto these new media using the same technique as described above for growth comparison on different media. To determine if a more gradual increase in peptone would correlate with a gradual secretion of melanin, we took the base media of MEA (solid) and changed the concentration of peptone to: 0.1%, 0.5%, 1%, 1.5%, 2%, 2.5%, 3%, 3.5%, 4%, and 5%. We then spotted 5 µL of both species onto the plates after performing a 10x serial dilution up to 10,000x dilution. The plates were grown at 23° for 10 days with a 12 hr light/dark cycle.

Albino mutant experiments:

Creation of EMS mutants and annotation of their mutations

Genetic modification of these species has not been established yet. However, random mutagenesis via chemical mutagens was performed in the hopes of finding albino mutants, to provide greater insight into the regulation of melanin production. UV exposure which is used frequently as a mutagen for random mutagenesis was attempted, but never resulted in phenotypically distinct mutants or albino mutants. Instead, we used ethyl methyl sulfonate to induce G:C to A:T mutations randomly within the genomes of our species. This was performed using the method by (Winston, 2008). Albino mutants and other interesting pigmentation or morphological mutants were isolated from the resulting mutagenesis, and their DNA was extracted using the same CTAB extraction manner stated above. Their DNA was then sent to the Microbial Genome Sequencing Center (MiGS) for genome re-sequencing and base-called

against the wild-type DNA. Resulting mutations were then manually annotated using the JGI Mycocosm genome "search" tool to determine if any genes were disrupted by the mutations to cause the phenotype observed.

Recovery of melanin production in albino mutants

Following recovery of our albino mutant, we attempted to restore melanin production via chemical induction of the other melanin biosynthetic pathways. We did this using hydroxyurea (HU) and L-DOPA. Hydroxyurea has been shown to enhance melanin production in *E. dermatitidis*, and L-DOPA is needed for certain fungi to produce melanized structures (Dadachova et al., 2007; Schultzhaus et al., 2020). Both YPD and MEA medium was made up and 20 mM of HU, 1 mM of L-DOPA, or 1 mM of 1,8-DHN was added to the medium after autoclaving. Our albino mutants were then grown up in the same way as our wild type cells. 5 µL of grown cells were spotted onto these media with added compounds and they were grown for 10 days at 23° C 12 hr light/dark cycle.

Results

Description of *Exophiala viscosium* and *Exophiala limosus*

Exophiala viscosium was isolated from Jackman Flats Provincial Park in B.C. Canada. Initial ITS sequencing was performed to obtain potential taxonomic matches. BLAST results to its ITS sequence matched 97.57% to "*Exophiala nigra* strain CBS 535.95" accession number: MH862481.1. Whole genome sequencing and further phylogenetic analyses subsequently revealed that *E. viscosium* is a novel species closely related to *E. sideris*.

Morphological characterization of *E. viscosium* demonstrated that compared to *E. dermatitidis*, *E. viscosium* has much darker pigmentation, and is also a more viscous cell culture. When scraping a colony off the plate it comes up like stretchy tar usually leaving a string of cells hanging off the sterile loop. *E. viscosium* does not disperse in water easily when re-suspending, but it does pellet easily at 10,000x g for 1 minute. When grown up on a MEA plate for a week or more, it will begin to form a rainbow sheen like an oil slick (**Figure 2A**). Hyphal growth will begin to form into the agar when the plate is left alone at room temperature for more than three weeks. Interestingly, secretion of melanin into the agar can be observed after two weeks on MEA and one week on YPD plates. In liquid culture, this occurs more quickly, with melanin observed in the supernatant starting at 5 days in MEA and 3 days in YPD. The cellular morphology of *E. viscosium* is that of a true yeast. It has large tear-drop shaped cells that usually bud one at a time but can sometimes bud 2-3 times simultaneously (**Figure 2B**). Lipid bodies are frequently observed, as the large circles within cells (**Figure 2B**), and have been confirmed by Nile red staining (data not shown). This isolate grows to its maximum density in 7 days at 23° C in 25 mL of MEA in a 250 mL Erlenmeyer flask shaken at 200 rpm. *Exophiala viscosium* was originally referred to as "Goopy" due to the nature of its morphology. Accordingly, we have formally named it *Exophiala viscosium* for the Latin term of viscous.

Exophiala limosus was isolated from a biological soil crust on public land in B.C. Canada. The ITS region of *E. limosus* most strongly matched "*Exophiala nigra* strain CBS 535.95" accession number: MH862481.1 with an identify of 97.67%. Although both *E. viscosium* and *E. limosus* have similar phylogenetic placement, their cellular morphology and budding patterns differ drastically (**Figure 2** and **Figure 4**). As seen in **Figure 2D**, the cellular morphology of *E. limosus'* resembles that of *Horatea*

werneckii as observed by Mitchison-Field et al. (2019). Cells are more elongated than *E. viscosium*, and when grown up to maximum density pipetting becomes difficult due to large clumps of cells formed by its more filamentous growth pattern. Both isolates have the consistency of sticky black tar, and an iridescent shine that forms after a week on an MEA plate. *Exophiala limosus* also fails to easily disperse when suspended in water but can be readily pelleted. These observations and the prominence of lipid bodies within the cells (**Figure 2D**) suggests that lipid-derived compounds could cause their sticky, water repelling, iridescent nature. This isolate grows to its maximum density in 7 days at 23° C in 25 mL of MEA in a 250 mL Erlenmeyer flask shaken at 200 rpm. Originally, *E. limosus* was named "Slimy" to reflect its colony characteristics. Accordingly, we have formally named it *Exophiala limosus* for the Latin term of muddy. Notably, *E. limosus* possesses a looser pellet and is less refractory to re-suspension than *E. viscosium*.

Genome description

The genome assembly sizes of these two novel *Exophiala* species are: 28.29 Mbp for *E. viscosium* and 28.23 Mbp for *E. limosus* (**Table 4**). These sizes are similar to other yeasts in the genus *Exophiala*, and are only a bit smaller than their closest relative *E. sideris* (29.51 Mbp). Although the genomes are smaller than *E. sideris*, predicted gene content is relatively higher; 11344 for *E. viscosium* and 11358 for *E. limosus* as compared to 11120 for *E. sideris* (**Table 4**). However, *E. sideris* appears to possess longer genes, transcripts, exons, and introns compared to *E. limosus* and *E. viscosium,* which could also contribute to the gene number to genome size differences (**Table 4**). *E. viscosium* contains the highest GC% amongst the *Exophiala* species listed in **Table 4**. *E. viscosium*'s GC content is even higher than *E. limosus* by 2.65%, which given their genetic similarities is quite interesting.

Mating type

Exophiala species are one of the many fungal genera whose mating capabilities remain incompletely understood and vary across the genus (Teixeira et al., 2017). The closest species to *E. viscosium* and *E. limosus* is *E. sideris,* within which both mating types have been characterized (Teixeira et al., 2017). Given the known order of genes in regions flanking the MAT locus in *Exophiala* species, we used comparative approaches to determine the mating identities of the sequenced *E. viscosium* and *E. limosus* isolates, and to look for possible evidence of homothallism. Homologues of the genes APN2, SLA2, APC5, COX13, and MAT1 (MAT1-1/alpha) in *E. viscosium* and *E. limosus* were identified via BLAST searches. We found that APN2 and SLA2 flank the MAT1-1 gene, and that both species contain the Herpotrichalleaceae-specific mating gene MAT1-1-4 (**Figure 3**). These results are not surprising, in that this is the exact same order of these genes in *E. sideris*. However, neither *E. viscosium* nor *E. limosus* contain an additional gene between APN2 and the MAT1-1-4 that is found in *E. sideris* (Teixeira et al., 2017). Furthermore, COX13 and APC5 are about 7,000bp downstream of the MAT locus in both species, but COX13 is on the opposite strand in *E. limosus* (**Figure 3**).

Phenotyping of *E. viscosium* and *E. limosus*:

To further understand the morphology, growth capabilities, and stress responses of *E. viscosium* and *E. limosus*, we performed multiple phenotyping experiments. The intent of these experiments was to

provide a broader perspective on the potential adaptations that would support the ability of these fungi to successfully colonize biological soil crusts and other extreme niches.

Budding patterns

Due to these species' similarities in colony morphology, observations of budding patterns in these new species became an essential task for differentiation. Microscopy was initially performed on cells grown from solid agar plates, which provided us with basic information that their cell morphology was different, with *E. viscosium* being very round and yeast-shaped and *E. limosus* having more elongated cells. But details regarding their budding patterns and cell polarity we're also needed. Using adapted protocols from (Mitchison-Field et al., 2019) we were able to perform a long-term microscopy time-lapse of the budding patterns of these species using the VALAP (1:1:1 Vasoline: Lanolin: Parafin) method to seal the edges of a coverslip while allowing gas exchange for cells to actively grow while observing for long periods of time (**Figure 4**). From this we were able to observe dramatic differences in the budding types of *E. viscosium* and *E. limosus*. *E. viscosium* buds with round cells in initially a distal fashion where the new bud forms 180° from the mother cell origination site, but also forms new buds at a ~90° angle from where the mother bud was formed in a proximal manner (**Figure 4; Video**). *E. limosus* on the other hand forms elongated cells in an exclusively distal manner, forming longer chains of cells instead of clusters (**Figure 4; Video**). These morphological differences in budding patterns influences the way these two species grow in a shaking flask. For example, *E. limosus* forms more elongated cells and buds distally which while does not create true hyphae, still creates larger clumps of cells which are not easily pipetted. However, *E. viscosium* since it forms rounder cells and buds with both distal and proximal patterns, does not form extensive clumps in a shaking flask and is more easily pipetted. *E. limosus* also forms more extensive biofilms at the liquid-air interface than *E. viscosium*, likely also due to the elongated cell morphology.

Growth of E. viscosium and E. limosus on 8 different medias:

Growth of *E. viscosium* and *E. limosus* on a variety of different media was done to assess growth requirements and their impact on pigmentation (**Figure 5**). The media used are described in **Table 1**, and include MAG, MEA, MN+NAG, MNV, PDA, Spider, YPD, and V8. The addition of Vitamin mix (Table 1) to any medium, but specifically to MAG and MN, caused the growth of both isolates to become much shinier, blacker (vs. browner), and more yeast-like. Growth on MEA causes the formation of a rainbow sheen, which is not seen on any other medium. Spider medium and YPD caused the formation of a dark-colored halo around colonies of both species. However, the halo around colonies grown on YPD is much darker and extends further than on Spider medium, and *E. viscosium* showed a more extensive halo than *E. limosus*. The ability of both species to grow on V8 medium implies that they can use cellulosic material as a carbon source. Overall, colony growth and pigmentation were similar across of media types for both species (**Figure 5**).

Carbon and nitrogen utilization

Carbon source utilization was determined using Biomerieux C32 carbon strips, which are typically used for identification of human pathogens (Tragiannidis et al., 2012). Following the protocols provided by the vendor, we were able to show that *E. viscosium* and *E. limosus* can utilize a wide range of carbon sources. Triplicates were performed on these strips to ensure results were uniform and representative. Overall, a variety of carbon sources supported robust growth of both species (e.g., D-glucose, L-sorbose,

D-galactose, N-acetyl glucosamine, D-sorbitol, D-xylose, glycerol, L-rhamnose, L-arabinose, D-celliobiose, and maltose), and there are only a few quantitative differences in utilization patterns (**Figure 6; Table 5**). Carbon sources that could not support growth include D-rafinose, D-melibiose, methyl-aD-glucopyranoside, and D-lactose. Both species were resistant to cycloheximide and were capable of producing a black color in the presence of esculin ferric citrate (**Figure 6**). Notably, for both *E. viscosium* and *E. limosus*, growth on some carbon sources, particularly sorbose and N-acetyglucosamine, lead to enhanced pigmentation (**Figure 6**).

We were particularly interested in patterns of nitrogen utilization for *E. viscosium* and *E. limosus* given their isolation from a nutrient deplete niche. Nine different nitrogen sources were tested: five amino acids (aspartate, glutamate, glycine, proline, serine), ammonium tartrate, sodium nitrate, urea, peptone (mixed short chain amino acids) as a positive control, and no nitrogen as a negative control. Both species are incapable of utilizing Aspartate and Glutamate as nitrogen sources (**Figure 7**). Preferred nitrogen sources for both species include ammonia and proline. However, they differ in that *E. viscosium* also prefers urea while *E. limosus* also prefers serine (**Figure 7**). Otherwise, patterns of nitrogen utilization appear generally similar across both species.

Optimal Growth Temperature and Range of growth temperatures

E. viscosium and *E. limosus* were isolated from an environment that experiences wide seasonal and diurnal temperature changes. As such, we wanted to determine both the optimal growing temperature for these species, as well as the limits at which they are capable of survival. Both isolates were serial diluted and spotted onto MEA plates to determine the carrying capacity at different temperatures. Both *E. viscosium and E. limosus* were capable of growth at 4° C, 15° C, 23° C, and 27° C, but could not grow at 37° C and 42° C (**Figure 8**). Optimal growth temperature of both *E. viscosium* and *E. limosus* was 23° C (**Figure 8**). Growth at 4° C was slow, but after a year the isolates both species formed obvious colonies and flooded the agar with melanin (**Figure 9**). Although neither species grew at 37° C, they retained viability as they were able to resume growth following return to 23° C after three days exposure to 37° C (**Figure 9**). In contrast, a similar experiment showed that incubation at 42° C is lethal.

UV and metal resistance

Melanized fungi are recognized for their resistance to UV light , and the possibility of using ionizing radiation as an energy source (Dadachova et al., 2007). To assess the response of *E. viscosium* and *E. limosus* to UV radiation, they were each exposed to a dose (120 seconds of 10,000 $\mu J/cm^2$) that was lethal to *S. cerevisiae* and *E. dermatitidis* (data not shown). The same level of exposure did not kill either *E. viscosium* or *E. limosus* (**Figure 10**), but did significantly reduce the number of viable colonies. Strikingly, surviving colonies showed no evidence of induced mutagenesis based on the absence of altered morphologies or pigmentation (**Figure 10**).

Polyextremotolerant fungi have been previously noted as having increased metal resistances as a result of their melanized cell wall and other adaptations to harsh environments (Gadd & de Rome, 1988). To test if these two new *Exophiala* spp. possess increased metal resistances when compared to *E. dermatitidis* and *S. cerevisiae*, we impregnated Whatman filter discs with various metals of different concentrations. Diameters of zones of clearing revealed no evidence for enhanced metal resistance in *E. viscosium* or *E. limosus* (**Table 6**). On the other hand, both species appear to be moderately more sensitive to $NiCl_2$ and $CdCl_2$ (**Table 6**).

Lipid Profiles

Both *E*. *viscosium* and *E*. *limosus* appear to possess abundant lipid bodies (**Figure 2**). This observation along with the unique sticky morphology of both species led us to the idea that they might contain unique or copious amounts of lipids. We performed a lipid extraction followed by thin layer chromatography (TLC) to observe patterns of lipid accumulation in *E. viscosium* and *E. limosus* grown on media that contained fermentable or non-fermentable sugars, both with high nitrogen and low nitrogen. These iterations creating four unique medias would allow us to cover as much of a spread of lipid changes as possible. S. *cerevisiae* and *E. dermatitidis* were also similarly analyzed. Results from this lipid extraction showed that our two new species did not seem to produce any unique or novel amounts or types of lipids when compared to *S. cerevisiae* and *E. dermatitidis* (**Figure 11**).

Melanin production and regulation in E. viscosium and E. limosus

Melanin biosynthesis gene annotation

A defining feature of black yeasts such as *E*. *viscosium* and *E*. *limosus* is their pigmentation due to the accumulation of melanin (Bell & Wheeler, 1986). Given the presumed importance of melanin to a polyextremotolerant lifestyle, we are interested in understanding how melanin production is regulated in response to environmental inputs. A first step in this process is to determine the types of melanin that *E*. *viscosium* and *E*. *limosus* are capable of producing. To accomplish this, the sequenced genomes of E. viscosium and E. limosus were annotated using protein sequences for all three melanin biosynthetic pathways in *Aspergillus niger* (Teixeira et al., 2017). The list of *A. niger* genes and their homologs in both *E. viscosium* and *E. limosus* are summarized in **Table 7**. Manual annotation and reverse BLASTP of melanin biosynthesis pathway genes showed that both *E. viscosium* and *E. limosus* have the capability to produce all three forms of known fungal melanins: DOPA melanin (pheomelanin), DHN melanin (allomelanin), and L-tyrosine derived pyomelanin.

Regulation of Melanin production using chemical blockers

Because *E*. *viscosium* and *E*. *limosus* possess the capability to produce all three forms of fungal melanin, we asked whether they were all being produced simultaneously or if one was preferred for production and secretion. We used chemical blockers for both DOPA melanin and DHN melanin to determine the predominant type of melanin produced on MEA and YPD. Kojic acid blocks the production of DOPA melanin, whereas Phthalide inhibits the synthesis of DHN melanin; both are effective at doses of 1, 10, and 100 µg/mL (Pal et al., 2014).

First, we used 100 mM of phthalide and 100 mg/mL of kojic acid in a filter dick assay. Placing drug-impregnated filter discs on freshly spread lawns of cells either individually or with both drugs combined did not block melanin production even though the concentrations of the drugs were higher than that of previous studies (**Figure 12**). Then using the highest dosage of 100 µg/mL, we added Phthalide and Kojic acid individually and combined to agar-solidified MEA, and both spread a lawn of cells and spotted serially diluted cells onto the plates. Neither assay resulted in blockage of melanin production in *E. viscosium* or *E. limosus* (**Figure 12**). However, addition of 100 µg/mL of Phthalide alone did result in their apparent secretion of a dark substance into MEA (**Figure 13**). Overall, inhibition of DOPA melanin or DHN melanin production did not qualitatively reduce colony pigmentation, potentially suggesting that the tyrosine-derived melanin is still being produced.

Melanin Secretion

The appearance of a dark pigment surrounding colonies of *E. viscosium* and *E. limosus* under specific conditions raised the possibility that these yeasts are able to secrete melanin into their local environment. The presence of dark pigments in the supernatants of liquid cultures lent further support to this idea.

Initial studies were performed to determine which media triggered the release of melanin. Both *E. viscosium* and *E. limosus* were capable of releasing the most melanin and in the shortest growth time on YPD, with *E. viscosium* seemingly secreting more than *E. limosus* (**Figure 4**). Because YPD and MEA only differ in yeast vs. malt extract as well as the percentage of peptone (2% in YPD, 0.2% in MEA), we first determined if the peptone differences impacted melanin secretion. By switching the peptone amounts in YPD and MEA, we demonstrated that *E. viscosium* acquired the ability to secrete melanin on MEA if it was supplemented with 2% peptone. To extend this observation, we added progressively higher amounts of peptone to MEA media (i.e., 10 different concentrations of peptone ranging from 0.1% to 5%). We observed that *E. viscosium* starts secreting melanin on MEA at a peptone amount of 2%, and *E. limosus* starts secreting melanin at about 4% peptone (**Figure 15**).

Confirmation of active melanin secretion from living cells

To confirm that the dark pigment in culture supernatants is indeed melanin, we performed a melanin extraction using previously described methods (Pal et al., 2014; Pralea et al., 2019). Although both enzymatic and chemical extraction of melanin was attempted, the chemical extraction process proved to be more efficient at recovering secreted melanin. (**Figure 16**). Therefore, all extractions going forward were performed using the chemical extraction method to ensure all melanin in the sample was precipitated out of the solution.

Growth of *E. viscosium, E. limosus,* and *E. dermatitidis* on YPD and MEA were observed daily for melanin secretion; 11 mL aliquots of their supernatant were removed daily and the melanin was extracted from each sample. As the experiment progressed, it was obvious that *E. viscosium* and *E. limosus* began secreting melanin on day 3 and secreted more in YPD than in MEA (**Figure 17**). *E. dermatitidis* on the other hand seemed to have a slower build-up of melanin, and melanin wasn't truly obvious in the medium until day 6 in MEA though it can be seen in MEA day 3 in **Figure 17**. Analysis of extracted melanin revealed that amounts increased over the course of the experiment, and that greater amounts of melanin are released in YPD for *E. viscosium* and *E. limosus* compared to MEA for *E. dermatitidis* (**Figure 16**). Interestingly, for both *E. viscosium* and *E. limosus*, their peak melanin secretion was on day 6 and not on day 7 (**Figure 18**). There was actually less melanin on day 7 for both species, indicating that the melanin after day 6 was either degrading, or was being taken back up by the cells. This was only obvious with reading the OD results of the extracted melanin, as the supernatants themselves day 5 and on were all strikingly dark and hard to differentiate visually (**Figure 17**). Extracted melanin from all *E. viscosium* and *E. limosus* samples also displayed the typical results from a full spectrum read on melanin, *E. dermatitidis* did not show typical melanin spectrum results until day 6 in YPD but were typical every day in MEA. When graphed with OD to Wavelength the sample should have an exponentially decreasing OD as wavelength increases, and when the OD is changed to a log scale, the full spectrum read should be a linear regression with an R^2 value of 0.97 or higher (Pralea et al., 2019). All *E. viscosium* and *E. limosus* samples displayed these features, and therefore we can confirm that the dark nature of their supernatants is caused by actively secreted melanin.

Genetic analysis of Melanin Production

Recovery of an albino mutant

At this time, molecular tools for the manipulation of *E. viscosium* and *E. limosus* are not yet available. Therefore, we combined classical genetics with genome re-sequencing to initially investigate the regulation of melanin production. Following mutagenesis with the alkylating agent ethyl methyl sulfonate (EMS), mutants following into four distinct phenotypic classes were recovered: pink, crusty, brown, and melanin over-secretion (Data not shown). The most intriguing of these phenotypes was the pink phenotype found in a mutant of *E. limosus* we called EMS 2-11 (**Figure 19**). It has already been shown that blockage of melanin production in *E*. *dermatitidis* by mutations in *pks1* results in pink instead of albino colonies because they also produce carotenoids that are normally masked by melanin and by-products such as flavolin (Geis & Szaniszlo, 1984; Geis et al., 1984). Genome re-sequencing of high molecular weight DNA from mutant EMS 2-11 and comparison to the reference E. limosus genome revealed a deleterious SNP causing a nonsense mutation in *pks1*. This mutation was on position 2,346,590 in scaffold 3, located in the *pks1* gene, which caused an C -> T mutation on the first position of the codon such that it became a stop codon. Interestingly, *pks1* only functions in one of the three melanin biosynthetic pathways found in *E*. *limosus*. Only two of the other random mutations found in EMS 2-11 were missense or nonsense mutations. One is a mutation in a transcriptional repressor EZH1, and another is in alcohol dehydrogenase GroES-like/Polyketide synthase enolreductase. Although either of these mutations could contribute to the pink phenotype, it is more likely that a nonsense mutation in *pks1* is solely responsible for the loss of melanin production despite the apparent presence of the other biosynthetic pathways.

Recovery of melanin production in albino mutant

Pks1 is a polyketide synthase gene that is essential for the first step in the DHN-melanin/Allomelanin production pathway. To test if “activation” of an alternative melanin production pathway could restore melanin production to the EMS 2-11 mutant, we substituted 1 mM of L-DOPA into the medium. As L-DOPA is a required external metabolite for melanin production in other fungi such as *Cryptococcus neoformans*, thus presumed that it would be taken up by our EMS 2-11 mutant and activate the DOPA melanin/pheomelanin biosynthesis pathway (Dadachova et al., 2007). However, substitution of 1 mM L-DOPA into either MEA or YPD was not enough to cause melanin production in the EMS 2-11 pks1 mutant (**Figure 19**). These plates were grown in the dark for 10 days, as L-DOPA will auto polymerize into a melanin precursor in the presence of light, and still no melanin production was observed. Hydroxyurea is another compound that in other *Exophiala* species induces melanin production, however addition of 20 mM of Hydroxyurea also did not activate melanin production in our EMS 2-11 albino mutant (**Figure 19**) (Schultzhaus et al., 2020). Finally, we substituted in 1 mM of 1,8-DHN into their media which is the immediate precursor to DHN melanin, in hopes of recovering melanin production. This resulted in recovery of melanized colonies, while on MEA they do not form extensive growth, their cells are still dark, and on YPD active dark colony growth is observed (**Figure 19**).

Discussion

A major limitation to our understanding of the role(s) played by BSCs in semi-arid ecosystems is our lack of insight into the components of these "biofilms" and the nature of their functional interactions. As photoautotrophs, the roles of cyanobacteria and algae in BSCs are clear (REF), but the importance of other residents such as fungi and bacteria is less so. Here, we identify two novel species of black yeasts from BSCs; *E. viscosium* and *E. limosus*. In addition to presenting the complete annotated genome sequence for each species, we also provide a relatively detailed profile of their ability to utilize diverse carbon and nitrogen sources, as well as their response to different forms of stress. Most importantly, we demonstrate that *E. viscosium* and *E. limosus* are capable of producing multiple types of melanin, including one that is secreted at high levels. Our results suggest that by making melanin available as a public good, black yeasts provide a critical service to the broader BSC community.

Description and genome features of E. viscosium and E. limosus

Exophiala viscosium and *E. limosus* are two novel fungi from the family Herpotrichielleaceae that we isolated from a lichen-dominated BSC. Since their initial isolation, their distinguishing features that lead us to investigate further were their "goopy" and "slimy" morphology, their impressively dark cells, their secretion of dark material into their growth medium, and their uniquely yeast-like morphology compared to more filamentous growth of other isolates. These unique aspects made them some of the easiest isolates to work with, accelerating their experiments faster than other isolated species (25 in total). However, until they were whole genome sequenced it was difficult to gain a deep understanding of what they were capable of physiologically and ecologically. With their genomes and many phenotyping experiments, we gained a basic idea of what these species are capable of in an ecological and fungal manner.

One interesting feature that the genome comparisons of *E. sideris* to *E. viscosium* and *E. limosus* revealed was that *E. sideris* contains a lower predicted gene content than the other two isolates. This could be a factor of their differences in their ecology and lifestyles. *E. sideris* was isolated from a highly toxic environment containing arsenate, hydrocarbons, and other toxins meaning this species had to specialize in withstanding these toxins rather than generalizing its survival genetic toolbox (Seyedmousavi et al., 2011). Additionally, the mating loci of these species are very similar containing only one mating type, MAT-alpha (MAT1-1), and the same gene organization within the loci albeit with different transcription directionality for COX13 and APC5 amongst the species. One mating type per genome is typical of many *Exophiala* species as most are heterothallic and maintain their anamorphic nomenclature of *Exophiala* (Teixeira et al., 2017; Untereiner & Naveau, 1999).

Phenotypic characterization of E. viscosium and E. limosus

These species have quite a flexible metabolism for carbon and nitrogen utilization. *E. viscosium* and *E. limosus* are capable of using 24 and 26 out of the 30 carbon sources respectively. Utilization of these carbon sources tested either completely or variably, including mannitol, ribitol, and glucose which are considered the main carbon sources exchanged within lichens (Richardson et al., 1967; Yoshino et al., 2020). They were also able to use all nitrogen sources provided, except both glutamate and aspartate were unfavorably used as opposed to what is seen at least in *S. cerevisiae*, where glutamate is a more favorable nitrogen source used for multiple core metabolism and amino acid production processes (Ljungdahl & Daignan-Fornier, 2012). Since peptone is their second most favorable nitrogen source, it is assumed that these species can import peptides and degrade them for sources of ammonium. Their most favorable nitrogen source is ammonium/ammonia though, which in their ecological environment

779 would likely be produced by cyanobacteria and other nitrogen-fixing bacteria (Belnap, 2002). However,
780 they can also use nitrate and urea as nitrogen sources, again pointing to their metabolic flexibility in
781 their nutrient deplete ecosystem.

782 Biological soil crusts in addition to their nutrient replete conditions, are also highly stressful
783 environments abiotically. These isolates came from a site that can experience extremes in temperature,
784 UV, and soil wetness/osmotic pressure. We determined that their optimal growth range is from 15° C to
785 27° C, however they are capable of slow growth at 4° C and while they do not grow at 37° C, they also do
786 not die at these temperatures after 72 consecutive hours of exposure. Their ability to continue growth
787 at 4° C is quite a feat though, and emphasizes their need to grow in unfavorable conditions if nutrients
788 and hydration are optimal. Wide range in growth temperatures, especially into the lower ranges, allows
789 for a longer time period of active growth in the arctic tundra as compared to growth in a hot desert
790 (Belnap, 2002).

791 As for resistance to UV light, both species were both highly capable of surviving the high exposure used
792 and were uniquely resistant to typical UV mutagenesis. Whether these species rely on their melanin for
793 resistance to DNA damage from UV, or because of their habitat, they evolved to have increased DNA
794 damage repair mechanisms will be a topic to investigate in the future.

795 Finally, two features we expected to find in our new species but we did not necessarily observe were
796 higher metal resistance and increased lipid accumulation. Melanin is known to enhance resistances to
797 metals (Bell & Wheeler, 1986; Gadd, 1994; Gorbushina, 2007; Purvis et al., 2004), and so it was assumed
798 that these new species would have increased metal tolerance when compared to non-melanized fungi.
799 However, of the metals tested, only $AgNO_3$ and $CuCl_2$ showed a decreased zone of clearing in *E.*
800 *viscosium* and *E. limosus*, compared to *S. cerevisiae* and *E. dermatitidis*. This result is understandable as
801 melanin has a higher affinity for copper due to the phenolic compounds it contains (Gadd & de Rome,
802 1988). As for lipid accumulation, we initially observed that both fungi produced lipid bodies confirmed
803 with Nile red staining. However, after performing our experiment comparing *S. cerevisiae*, *E.*
804 *dermatitidis*, *E. viscosium*, and *E. limosus* lipid production we did not observe a difference in lipid
805 amounts per cell count.

806 *Secretion of melanin by E. viscosium and E. limosus*

807 Melanin is considered an expensive secondary metabolite to produce by organisms, since it is made up
808 of conglomerates of polyphenols and as such contains many carbons. Therefore, it would be assumed
809 that an organism would not want to create melanin just to export it out of the cell unless there was a
810 beneficial reason behind it. Additionally, there are not many fungi that are known to secrete melanin
811 and none in the genus *Exophiala*, so the possibility of novel species that secrete melanin into their
812 surroundings was intriguing. Both novel fungi have the genetic tools to produce all three types of fungal
813 melanin: allomelanin, pyomelanin, and eumelanin; but it is still unknown how these melanin
814 biosynthetic pathways are regulated, and which are being actively produced.

815 In our attempts to understand the regulation of melanin production by *E. viscosium* and *E. limosus* we
816 tried blocking individual pathways using known chemical blockers of DHN and DOPA melanin, phthalide
817 and kojic acid respectively. Neither blockers, nor their combination at the highest amounts used were
818 able to block the production of melanin in either species. If these species have the capability to produce
819 all three melanins, then it is possible that they are producing more than one at the same time. This

could be the case here, since the combination of both kojic acid and phthalide still resulted in melanized cells which would indicate that pyomelanin was the cause of melanization.

Linked regulation of multiple forms of melanin was observed with our EMS mutant where the pks1 gene contained a nonsense mutation. Although pks1 is the first enzyme involved in only the production of DHN-derived allomelanin, the cells that resulted from this mutation were all albino. Theoretically, these cells should have still been capable of producing the two other melanins as their pathways were not disrupted by any mutations, but this was not the case. Therefore, it is possible that either these fungi are only producing DHN-derived allomelanin and disruption of the pks1 gene causes all melanin production to shut down, or that pks1 (or downstream creation of allomelanin) is essential for the regulation of other melanin productions.

Additionally, we wanted to confirm that these fungi were actively secreting melanin while alive. In our experiments melanin began to accumulate starting as early as day 2, therefore we could confirm that it is live cells that are secreting melanin and not dead lysed cells. However, we observed a decrease in melanin concentrations after day 6 in both YPD and MEA in *E. viscosium* and *E. limosus* which still poses an intriguing potential for melanin reabsorption or degradation by these species.

For *E. viscosium* and *E. limosus* the medium that stimulates the most melanin secretion is YPD which has 10x more nitrogen (2% vs. 0.2%) than the alternative medium we use, MEA, which neither fungi secrete melanin into when plated on solid media. This led us to believe that nitrogen amount could potentially have an effect on the production of secreted melanin, which we did observed as we increased peptone amounts in the medium. Although *E. viscosium* required less peptone *than E. limosus* to being secreting melanin. Interestingly, the only fungal melanin that has nitrogen in its precursor structure is the DOPA derived pheomelanin. This was one of two melanins that would have been allowed to be produced in the presence of phthalide, which we observed also induced the secretion of melanin in these fungi. This provides support that the secreted melanin is either pheomelanin, as it requires more nitrogen in order to be produced, or that the production of pheomelanin (DOPA) and the water soluble pyomelanin (Turick et al., 2010) are linked.

Insights into polyextremotolerant fungi's niche within the biological soil crust consortium

Fungi living amongst lichens, within an even larger more diverse consortium is an odd ecological niche to hold. These fungi are likely not associated directly with the lichens themselves, yet are surrounded by algae, cyanobacteria, and other bacteria in the same way that a lichenized-fungus is surrounded by a similar community of microbes. So why not lichenize? Why stay as a free-living fungus? Members of the genus *Exophiala* (Family Herpotrichiellaceae) are phylogenetically related to the lichen-forming Verrucariales, and reside between Lecanoromycetes and Lichinomycetes (James et al., 2006). Lifestyle changes within Eurotiomycetes contributed to the polyphyletic nature of lichenization within the Ascomycetes, but since surrounding taxa are lichenized it is more likely that these species lost lichenization than three distinct lichenization events within closely related species (Lutzoni et al., 2001). Possibly, because these new *Exophiala* species have lichenized ancestors, they lost their "true lichenization" capabilities, but maintained the genetic tools to interact with algae, cyanobacteria, and other bacteria to form lichen-like symbioses. But these seemingly free-living yeasts could also be lichenicolus fungi, and only inhabiting the lichens formed in biological soil crusts. As these are two newly identified species, it will require more extensive molecular approaches to determine how ubiquitous these species are within biological soil crusts around the world or even within lichens.

Links between environmental nitrogen amounts and melanin secretion could have strong implications for interactions between these fungi and their nitrogen fixing community members. Increase in nitrogen caused increase in melanin secretion, increase in nitrogen in a biological soil crust would have to come from nitrogen-fixers such as cyanobacteria, other bacteria, and archaea in the community. Therefore, as the n-fixers provide the fungal cells with ammonia, their secreted melanin increases and helps assist the community in abiotic protection. This could be a factor of the window of opportunity for the biological soil crust community to actively respire and grow requires exact temperatures and exact hydration, but not exact UV exposure. In the event that optimal growth conditions occur for this community to grow, UV exposure will always be the constant drawback. One way of ensuring the community (and therefore the individual) survives in this circumstance, is blocking UV overexposure by secretion of melanin into the biofilm. Alternatively, or simultaneously, this secreted melanin could be an external source of carbon used by the fungi and possibly others when the environment does not allow for photosynthesis. As stated, melanin is an expensive bioproduct carbon-wise, and secretion of such an expensive product seems wasteful. However, if these fungi are either capable of shielding the greater biological soil crust community and/or creating an external carbon storage for less-than-ideal conditions, this could be an optimal usage of secreted melanin.

Through the use of genome annotations, extensive phenotyping, and melanin regulation tests we have derived certain important features that we believe are vital to the survival of these species in their ecosystem. We believe that these two fungi and fungi related to them have an important niche for the biological soil crust community. Their ability to produce melanin whether it be in their cell wall directly or secreted, allows for an increase in the overall protection of the rest of the community via this melanin good. Melanin is likely a vital commodity for the biological soil crust community to thrive amongst the abiotic extremes their ecosystem provides, and having a consortium of polyextremotolerant fungi there to produce it is essential for the survival of the community. Additional questions that still need to be answered are: how is the production of different types of melanin regulated in response to environmental and chemical inputs?; what role does secreted melanin play in the BSC community – is it a shared public good?; and can the genome sequences be leveraged to further understand how these yeasts interact with other members of the BSC community?

Citations:

Ametrano, C. G., Selbmann, L., & Muggia, L. (2017). A standardized approach for co-culturing Dothidealean rock-inhabiting fungi and lichen photobionts in vitro. *Symbiosis*, *73*(1), 35-44.

Armaleo, D., Müller, O., Lutzoni, F., Andrésson, Ó. S., Blanc, G., Bode, H. B., . . . Xavier, B. B. (2019). The lichen symbiosis re-viewed through the genomes of Cladonia grayi and its algal partner Asterochloris glomerata. *BMC Genomics*, *20*(1), 605. https://doi.org/10.1186/s12864-019-5629-x

Bates, S. T., Garcia-Pichel, F., & Nash III, T. (2010). Fungal components of biological soil crusts: insights from culture-dependent and culture-independent studies. *Bibliotheca Lichenologica*, *105*, 197-210.

Bates, S. T., Reddy, G. S., & Garcia-Pichel, F. (2006). Exophiala crusticola anam. nov.(affinity Herpotrichiellaceae), a novel black yeast from biological soil crusts in the Western United States. *International journal of systematic and evolutionary microbiology*, *56*(11), 2697-2702.

Bell, A. A., & Wheeler, M. H. (1986). Biosynthesis and functions of fungal melanins. *Annual review of phytopathology*, *24*(1), 411-451.

Belnap, J. (2002). Nitrogen fixation in biological soil crusts from southeast Utah, USA. *Biology and fertility of soils*, *35*(2), 128-135.

Belnap, J. (2003). The world at your feet: desert biological soil crusts. *Frontiers in Ecology and the Environment*, *1*(4), 181-189.

Belnap, J., Büdel, B., & Lange, O. L. (2001). Biological soil crusts: characteristics and distribution. In *Biological soil crusts: structure, function, and management* (pp. 3-30). Springer.

Belnap, J., & Eldridge, D. (2001). Disturbance and recovery of biological soil crusts. In *Biological soil crusts: structure, function, and management* (pp. 363-383). Springer.

Bowker, M. A., Reed, S., Belnap, J., & Phillips, S. (2002). Temporal variation in community composition, pigmentation, and Fv/Fm of desert cyanobacterial soil crusts. *Microbial Ecology*, 13-25.

Bowker, M. A., Soliveres, S., & Maestre, F. T. (2010). Competition increases with abiotic stress and regulates the diversity of biological soil crusts. *Journal of Ecology*, *98*(3), 551-560.

Cao, W., Zhou, X., McCallum, N. C., Hu, Z., Ni, Q. Z., Kapoor, U., . . . Mantanona, A. J. (2021). Unraveling the structure and function of melanin through synthesis. *Journal of the American Chemical Society*, *143*(7), 2622-2637.

Cordero, R. J., & Casadevall, A. (2017). Functions of fungal melanin beyond virulence. *Fungal Biology Reviews*, *31*(2), 99-112.

Cubero, O. F., Crespo, A., Fatehi, J., & Bridge, P. D. (1999). DNA extraction and PCR amplification method suitable for fresh, herbarium-stored, lichenized, and other fungi. *Plant Systematics and Evolution*, *216*(3), 243-249.

D'Orazio, J., Jarrett, S., Amaro-Ortiz, A., & Scott, T. (2013). UV radiation and the skin. *International journal of molecular sciences*, *14*(6), 12222-12248.

Dadachova, E., Bryan, R. A., Huang, X., Moadel, T., Schweitzer, A. D., Aisen, P., . . . Casadevall, A. (2007). Ionizing radiation changes the electronic properties of melanin and enhances the growth of melanized fungi. *PloS one*, *2*(5), e457.

De Hoog, G., Vicente, V., Caligiorne, R., Kantarcioglu, S., Tintelnot, K., Gerrits van den Ende, A., & Haase, G. (2003). Species diversity and polymorphism in the Exophiala spinifera clade containing opportunistic black yeast-like fungi. *Journal of Clinical Microbiology*, *41*(10), 4767-4778.

Donlan, R. M., & Costerton, J. W. (2002). Biofilms: survival mechanisms of clinically relevant microorganisms. *Clinical microbiology reviews*, *15*(2), 167-193.

Frases, S., Salazar, A., Dadachova, E., & Casadevall, A. (2007). Cryptococcus neoformans can utilize the bacterial melanin precursor homogentisic acid for fungal melanogenesis. *Applied and environmental microbiology*, *73*(2), 615-621.

Gadd, G. M. (1994). Interactions of fungi with toxic metals. *The Genus Aspergillus*, 361-374.

Gadd, G. M., & de Rome, L. (1988). Biosorption of copper by fungal melanin. *Applied microbiology and biotechnology*, *29*(6), 610-617.

Geis, P. A., & Szaniszlo, P. J. (1984). Carotenoid pigments of the dematiaceous fungus Wangiella dermatitidis. *Mycologia*, *76*(2), 268-273.

Geis, P. A., Wheeler, M. H., & Szaniszlo, P. J. (1984). Pentaketide metabolites of melanin synthesis in the dematiaceous fungus Wangiella dermatitidis. *Archives of microbiology*, *137*(4), 324-328.

Gessler, N., Egorova, A., & Belozerskaya, T. (2014). Melanin pigments of fungi under extreme environmental conditions. *Applied Biochemistry and Microbiology*, *50*(2), 105-113.

Gnerre, S., MacCallum, I., Przybylski, D., Ribeiro, F. J., Burton, J. N., Walker, B. J., . . . Jaffe, D. B. (2011). High-quality draft assemblies of mammalian genomes from massively parallel sequence data. *Proceedings of the National Academy of Sciences*, *108*(4), 1513-1518. https://doi.org/10.1073/pnas.1017351108

952 Gorbushina, A. A. (2007). Life on the rocks. *Environmental microbiology*, *9*(7), 1613-1631.
953 Gostinčar, C., Grube, M., De Hoog, S., Zalar, P., & Gunde-Cimerman, N. (2009). Extremotolerance in
954 fungi: evolution on the edge. *FEMS microbiology ecology*, *71*(1), 2-11.
955 Gostinčar, C., Grube, M., & Gunde-Cimerman, N. (2011). Evolution of fungal pathogens in domestic
956 environments? *Fungal biology*, *115*(10), 1008-1018.
957 Gostinčar, C., Muggia, L., & Grube, M. (2012). Polyextremotolerant black fungi: oligotrophism, adaptive
958 potential, and a link to lichen symbioses. *Frontiers in Microbiology*, *3*, 390.
959 Grabherr, M. G., Haas, B. J., Yassour, M., Levin, J. Z., Thompson, D. A., Amit, I., . . . Zeng, Q. (2011). Full-
960 length transcriptome assembly from RNA-Seq data without a reference genome. *Nature*
961 *biotechnology*, *29*(7), 644-652.
962 Grigoriev, I. V., Nikitin, R., Haridas, S., Kuo, A., Ohm, R., Otillar, R., . . . Shabalov, I. (2014). MycoCosm
963 portal: gearing up for 1000 fungal genomes. *Nucleic Acids Research*, *42*(D1), D699-D704.
964 https://doi.org/10.1093/nar/gkt1183
965 Grube, M., Cernava, T., Soh, J., Fuchs, S., Aschenbrenner, I., Lassek, C., . . . Sensen, C. W. (2015).
966 Exploring functional contexts of symbiotic sustain within lichen-associated bacteria by
967 comparative omics. *The ISME journal*, *9*(2), 412-424.
968 Hayakawa, Y., Ishikawa, E., Shoji, J. y., Nakano, H., & Kitamoto, K. (2011). Septum-directed secretion in
969 the filamentous fungus Aspergillus oryzae. *Molecular microbiology*, *81*(1), 40-55.
970 Hom, E. F., & Murray, A. W. (2014). Niche engineering demonstrates a latent capacity for fungal-algal
971 mutualism. *Science*, *345*(6192), 94-98.
972 James, T. Y., Kauff, F., Schoch, C. L., Matheny, P. B., Hofstetter, V., Cox, C. J., . . . Miadlikowska, J. (2006).
973 Reconstructing the early evolution of Fungi using a six-gene phylogeny. *Nature*, *443*(7113), 818-
974 822.
975 Kirilovsky, D. (2010). The photoactive orange carotenoid protein and photoprotection in cyanobacteria.
976 *Recent advances in phototrophic prokaryotes*, 139-159.
977 Lan, S., Wu, L., Zhang, D., & Hu, C. (2012). Successional stages of biological soil crusts and their
978 microstructure variability in Shapotou region (China). *Environmental Earth Sciences*, *65*(1), 77-
979 88.
980 Lawrence, C. W. (1982). Mutagenesis in Saccharomyces cerevisiae. *Advances in genetics*, *21*, 173-254.
981 Ljungdahl, P. O., & Daignan-Fornier, B. (2012). Regulation of amino acid, nucleotide, and phosphate
982 metabolism in Saccharomyces cerevisiae. *Genetics*, *190*(3), 885-929.
983 Lutzoni, F., Pagel, M., & Reeb, V. (2001). Major fungal lineages are derived from lichen symbiotic
984 ancestors. *Nature*, *411*(6840), 937-940.
985 Maier, S., Muggia, L., Kuske, C. R., & Grube, M. (2016). Bacteria and non-lichenized fungi within
986 biological soil crusts. In *Biological Soil Crusts: An Organizing Principle in Drylands* (pp. 81-100).
987 Springer.
988 Mitchison-Field, L. M. Y., Vargas-Muñiz, J. M., Stormo, B. M., Vogt, E. J. D., Van Dierdonck, S., Pelletier, J.
989 F., . . . Gladfelter, A. S. (2019). Unconventional Cell Division Cycles from Marine-Derived Yeasts.
990 *Current Biology*, *29*(20), 3439-3456.e3435. https://doi.org/10.1016/j.cub.2019.08.050
991 Pal, A. K., Gajjar, D. U., & Vasavada, A. R. (2014). DOPA and DHN pathway orchestrate melanin synthesis
992 in Aspergillus species. *Medical mycology*, *52*(1), 10-18.
993 Perez-Cuesta, U., Aparicio-Fernandez, L., Guruceaga, X., Martin-Souto, L., Abad-Diaz-de-Cerio, A.,
994 Antoran, A., . . . Rementeria, A. (2020). Melanin and pyomelanin in Aspergillus fumigatus: from
995 its genetics to host interaction. *International Microbiology*, *23*(1), 55-63.
996 Pralea, I.-E., Moldovan, R.-C., Petrache, A.-M., Ilieș, M., Hegheș, S.-C., Ielciu, I., . . . Radu, M. (2019). From
997 extraction to advanced analytical methods: The challenges of melanin analysis. *International*
998 *journal of molecular sciences*, *20*(16), 3943.

Purvis, O. W., Bailey, E. H., McLean, J., Kasama, T., & Williamson, B. J. (2004). Uranium biosorption by the lichen Trapelia involuta at a uranium mine. *Geomicrobiology Journal*, *21*(3), 159-167.

Pócs, T. (2009). Cyanobacterial crust types, as strategies for survival in extreme habitats. *Acta Botanica Hungarica*, *51*(1-2), 147-178.

Płonka, P., & Grabacka, M. (2006). Melanin synthesis in microorganisms: biotechnological and medical aspects. *Acta Biochimica Polonica*, *53*(3).

Rajeev, L., Da Rocha, U. N., Klitgord, N., Luning, E. G., Fortney, J., Axen, S. D., . . . Kerfeld, C. A. (2013). Dynamic cyanobacterial response to hydration and dehydration in a desert biological soil crust. *The ISME journal*, *7*(11), 2178-2191.

Rastogi, R. P., Kumar, A., Tyagi, M. B., & Sinha, R. P. (2010). Molecular mechanisms of ultraviolet radiation-induced DNA damage and repair. *Journal of nucleic acids*, *2010*.

Richardson, D., Smith, D., & Lewis, D. (1967). Carbohydrate movement between the symbionts of lichens. *Nature*, *214*(5091), 879-882.

Rosas, Á. L., Nosanchuk, J. D., Gómez, B. L., Edens, W. A., Henson, J. M., & Casadevall, A. (2000). Isolation and serological analyses of fungal melanins. *Journal of immunological methods*, *244*(1-2), 69-80.

Schroeder, W. L., Harris, S. D., & Saha, R. (2020). Computation-driven analysis of model polyextremotolerant fungus exophiala dermatitidis: defensive pigment metabolic costs and human applications. *IScience*, *23*(4), 100980.

Schultzhaus, Z., Romsdahl, J., Chen, A., Tschirhart, T., Kim, S., Leary, D., & Wang, Z. (2020). The response of the melanized yeast Exophiala dermatitidis to gamma radiation exposure. *Environmental microbiology*, *22*(4), 1310-1326.

Seyedmousavi, S., Badali, H., Chlebicki, A., Zhao, J., Prenafeta-Boldu, F. X., & De Hoog, G. S. (2011). Exophiala sideris, a novel black yeast isolated from environments polluted with toxic alkyl benzenes and arsenic. *Fungal biology*, *115*(10), 1030-1037.

Teixeira, M. d. M., Moreno, L. F., Stielow, B., Muszewska, A., Hainaut, M., Gonzaga, L., . . . Souza, R. (2017). Exploring the genomic diversity of black yeasts and relatives (Chaetothyriales, Ascomycota). *Studies in mycology*, *86*, 1-28.

Tragiannidis, A., Fegeler, W., Rellensmann, G., Debus, V., Müller, V., Hoernig-Franz, I., . . . Groll, A. (2012). Candidaemia in a European Paediatric University Hospital: a 10-year observational study. *Clinical Microbiology and Infection*, *18*(2), E27-E30.

Turick, C. E., Knox, A. S., Becnel, J. M., Ekechukwu, A. A., & Milliken, C. E. (2010). Properties and function of pyomelanin. *Biopolymers*, *449*, 72.

Untereiner, W. A., & Naveau, F. A. (1999). Molecular systematics of the Herpotrichiellaceae with an assessment of the phylogenetic positions of Exophiala dermatitidis and Phialophora americana. *Mycologia*, *91*(1), 67-83.

White, T. J., Bruns, T., Lee, S., & Taylor, J. (1990). 38 - AMPLIFICATION AND DIRECT SEQUENCING OF FUNGAL RIBOSOMAL RNA GENES FOR PHYLOGENETICS. In M. A. Innis, D. H. Gelfand, J. J. Sninsky, & T. J. White (Eds.), *PCR Protocols* (pp. 315-322). Academic Press. https://doi.org/https://doi.org/10.1016/B978-0-12-372180-8.50042-1

Winston, F. (2008). EMS and UV mutagenesis in yeast. *Current protocols in molecular biology*, *82*(1), 13.13 B. 11-13.13 B. 15.

Yoshino, K., Yamamoto, K., Masumoto, H., Degawa, Y., Yoshikawa, H., Harada, H., & Sakamoto, K. (2020). Polyol-assimilation capacities of lichen-inhabiting fungi. *The Lichenologist*, *52*(1), 49-59.

Zanne, A. E., Abarenkov, K., Afkhami, M. E., Aguilar-Trigueros, C. A., Bates, S., Bhatnagar, J. M., . . . Crowther, T. W. (2020). Fungal functional ecology: bringing a trait-based approach to plant-associated fungi. *Biological Reviews*, *95*(2), 409-433.

Zerbino, D. R., & Birney, E. (2008). Velvet: algorithms for de novo short read assembly using de Bruijn graphs. *Genome research*, *18*(5), 821-829.

Zupančič, J., Novak Babič, M., Zalar, P., & Gunde-Cimerman, N. (2016). The black yeast Exophiala dermatitidis and other selected opportunistic human fungal pathogens spread from dishwashers to kitchens. *PLoS One*, *11*(2), e0148166.

Acknowledgements

The work conducted by the U.S. Department of Energy Joint Genome Institute, a DOE Office of Science User Facility, is supported by the Office of Science of the U.S. Department of Energy under Contract No. DE-AC02-05CH11231.

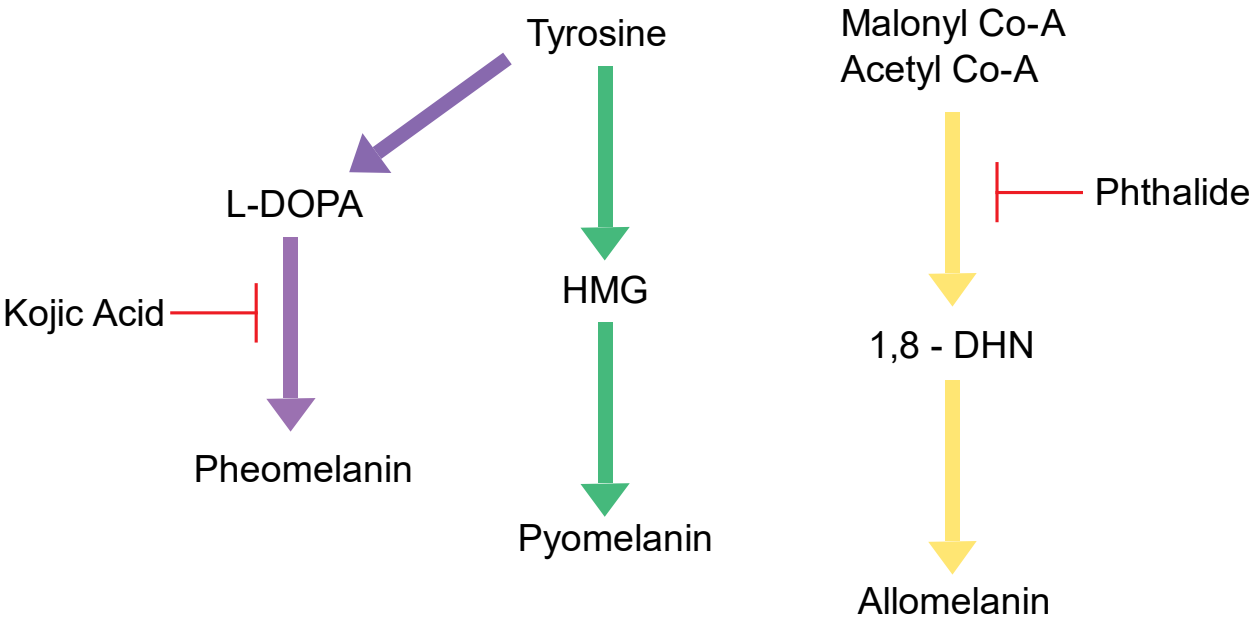

Figure 1: Visual summary of fungal melanin production and the chemicals that block each melanin pathway. Pheomelanin and Pyomelanin both use tyrosine as their starting reagent but have different biosynthesis pathways unrelated to each other. Pheomelanin uses L-DOPA as a precursor to the final melanin and pyomelanin uses HMG as a precursor. Allomelanin's starting components are malonyl co-A and acetyl co-A, and its immediate precursor is 1,8-DHN. Kojic acid is a chemical blocker that blocks production of pheomelanin, and phthalide blocks production of allomelanin.

Table 1: Medias used and their compositions

Media Name	**Acronym**	**Composition (L^{-1})**
Malt Extract Agar Glucose	MAG	20 g Dextrose 20 g Malt Extract 2 g Peptone 1 mL Hutner's Trace Elements 1 mL Vitamin Mix 15 g Agar
Malt Extract Agar	MEA	20 g Dextrose 20 g Malt Extract 2 g Peptone 15 g Agar
Minimal	MN	10 g Dextrose 50 mL 20x Nitrate salts 1 mL Hutner's Trace Elements
Minimal + Vitamins	MNV	10 g Dextrose 50 mL 20x Nitrate salts 1 mL Hutner's Trace Elements 1 mL Vitamin Mix to MN
Minimal + N-acetyl Glucosamine	MN+NAG	10 g Dextrose 50 mL 20x Nitrate salts 1 mL Hutner's Trace Elements

		4.74 g N-Acetyl Glucosamine (21.43 mM)
Potato Dextrose Agar	PDA	24 g Potato dextrose powder 15 g agar (if not in potato powder)
Spider	Spider	20 g Nutrient Broth 20 g Mannitol 4 g K_2HPO_4 27 g Agar pH adjusted to 7.2 with NaOH
Yeast Extract Peptone Dextrose	YPD	20 g Dextrose 20 g Peptone 10 g Yeast Extract 20 g Agar
V8	V8	200 mL V8 Juice 2 g $CaCO_3$ 15 g Agar
Additives	**Volume/L**	**Composition**
20X Nitrate Salts/MN salts	1 L	120 g $NaNO_3$ (remove for "MN salts") 10.4 g KCl 10.4 g $MgSO_4$-$7H_2O$ 30.4 g KH_2PO_4
Hutner's Trace Elements	100 mL	2.2 g $ZnSO_4$-$7H_2O$ 1.1 g H_3BO_3 0.5 g $MnCl_2$-$4H_2O$ 0.5 g $FeSO_4$-$7H_2O$ 0.17 g $CoCL_2$-$6H_2O$ 0.16 g $CuSO_4$-$5H_2O$ 0.15 g Na_2MoO_4-$2H_2O$ 5 g EDTA (Na_4)
Vitamin Mix	100 mL	10 mg biotin 10 mg pyridoxin 10 mg thiamine 10 mg riboflavin 10 mg p-aminobenzoic acid (PABA) 10 mg nicotinic acid

Table 2: Nitrogen Sources, Concentrations, and Providers

Nitrogen Source	**Concentration**	**Catalog number**
No Nitrogen	N/A	N/A
Peptone	1% w/v	Fisher Brand: BP1420
L-Proline	100 mM	Sigma: P-0380
Ammonium tartrate	100 mM	Sigma: A2956
L-Serine	100 mM	Sigma: S4500
Sodium Nitrate	100 mM	Fisher Brand: S343
Glycine	100 mM	Fisher BioReagents: BP381

L-Glutamic acid	100 mM	Sigma: G1251
L-Aspartic acid	100 mM	Sigma: A9256
Urea	50 mM	Alfa Aesar: A12360

Table 3: Metals used and their concentration

Metal	**Concentration**	**Catalog Number**
$FeSO_4$	1 M	Fisher: I146
$CoCl_2$	0.5 M	Sigma: C-2644
$NiCl_2$	1.5 M	Sigma-aldrich: 223387
$CuCl_2$	1.5 M	Sigma: 203149
$CdCl_2$	10 mM	Fisher: 7790-84-3
$AgNO_3$	0.47 M	Alfa Aesar: 7761-88-8

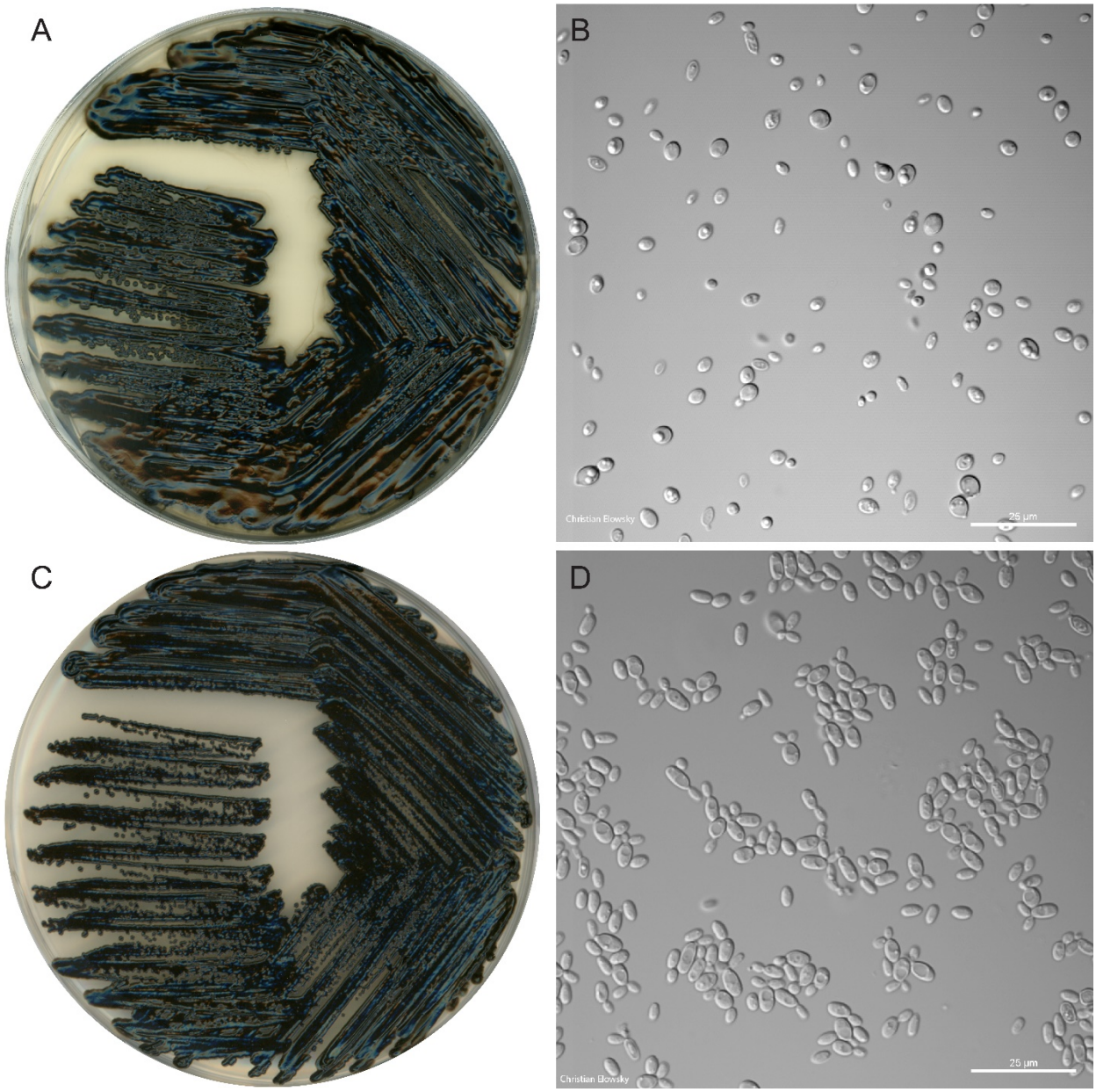

Figure 2: A) *E. viscosium* plate morphology; grown on an MEA plate for 10 days. *B) E. viscosium* cell morphology; grown in liquid MEA for 5 days; 60x objective lens. C) *E. limosus* plate morphology; grown on a MEA plate for 10 days. D) *E. limosus* cell morphology; grown in liquid MEA for 5 days; 60x objective lens. (Both plate photos and microscopy photos were taken by Christian Elowsky)

Table 4: Genome descriptions of the novel *Exophiala* species and close relatives

	E. viscosium	*E. limosus*	*E. sideris*	*E. spinifera*	*E. xenobiotica*	*E. oligosperma*	*E. dermatitidis*
Genome Assembly statistics							
Genome Assembly size (Mbp)	28.29	28.23	29.51	32.91	31.41	38.22	26.35

Sequencing read coverage depth	147.3x	147.8x	NA	NA	NA	NA	NA
Number of contigs	35	27	69	143	64	287	10
Number of scaffolds	30	17	5	28	15	143	10
Number of scaffolds >= 2Kbp	25	17	5	20	11	129	10
Scaffold N50	4	5	2	4	3	5	4
Scaffold L50 (Mbp)	2.24	2.89	7.9	3.79	5.04	3.39	3.62
Number of gaps	5	10	64	115	49	144	0
% of scaffold length in gaps	0.00%	0.00%	0.10%	0.10%	0.10%	0.80%	0.00%
Three largest Scaffolds (Mbp)	5.39, 4.56, 2.49	4.57, 3.58, 2.93	9.94, 7.90, 7.15	6.18, 3.93, 3.92	5.55, 5.20, 5.04	4.47, 4.29, 4.12	4.25, 4.22, 3.71
GC content (%)	51.91	49.26	49.73	49.42	51.89	50.99	51.74
Gene statistics							
Number of genes	11344	11358	11120	12049	13187	13234	9562
Gene length (bp, Average)	1840	1844	2044	1593	2072	2090	2237
Gene length (bp, Median)	1666	1671	1823	1415	1845	1879	1923
Transcript length (bp, Average)	1740	1746	1933	1483	1941	1949	2122
Transcript length (bp, Median)	1564	1574	1710	1311	1710	1735	1794
Exon length (bp, Average)	705	707	776	621	738	743	896
Exon length (bp, Median)	410	414	452	339	430	426	513
Intron length (bp, Average)	70	69	74	81	80	85	85
Intron length (bp, Median)	56	56	56	61	57	61	62
Protein length (aa, Average)	488	489	500	494	492	488	501
Protein length (aa, Median)	428	430	434	437	431	429	429
Exons per gene (Average)	2.47	2.47	2.49	2.39	2.63	2.62	2.37
Exons per gene (Median)	2	2	2	2	2	2	2

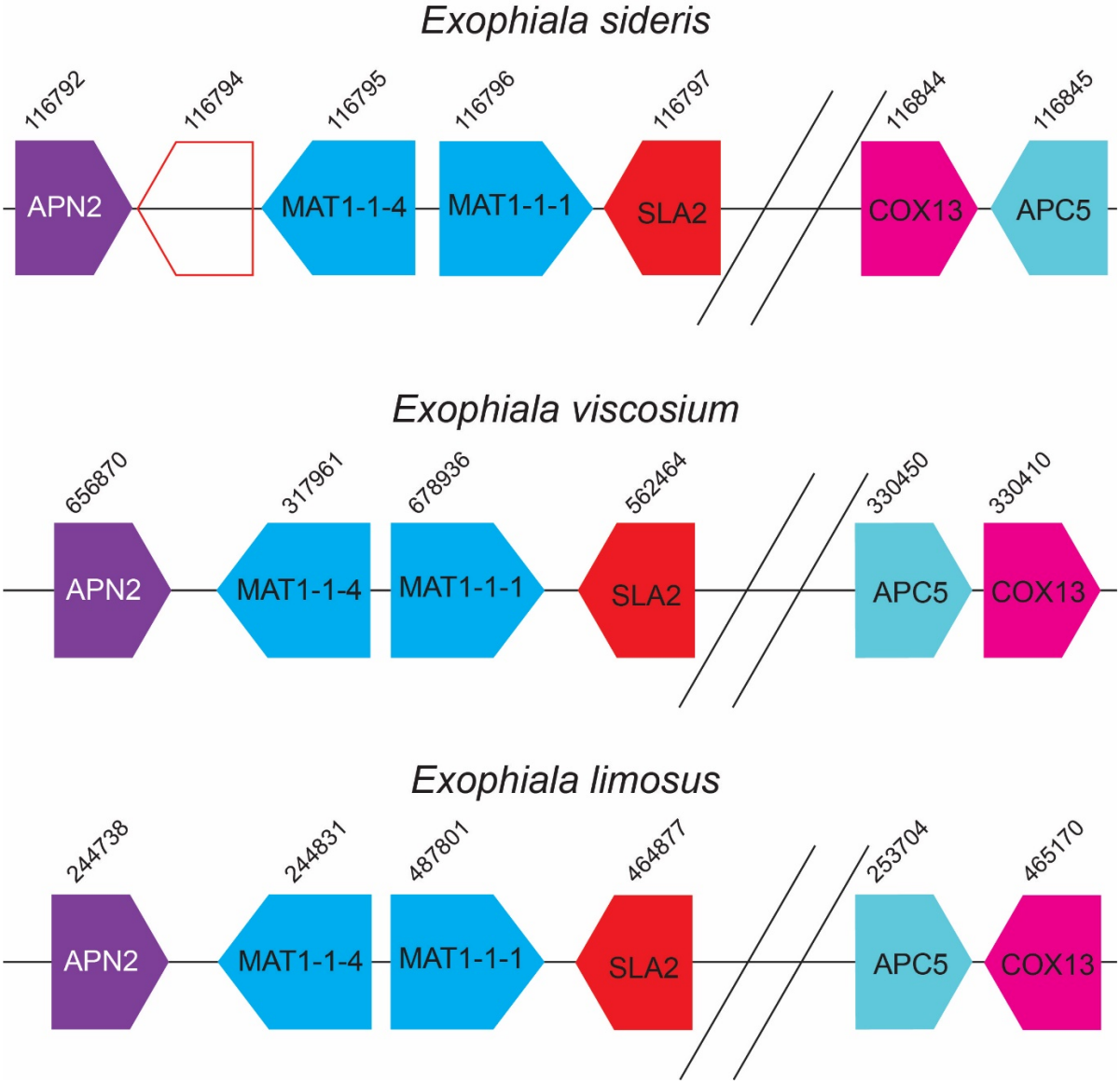

Figure 3: MAT loci gene order for *E. viscosium*, *E. limosus*, and *E. sideris*. In all three species the same genes are present within the MAT locus. *E. sideris* is indicated to have a hypothetical protein between APN2 and MAT1-1-4, whereas *E. viscosium and E. limosus* were not predicted to have that gene. Additionally, all three species have COX 13 and APC5 downstream of their mat loci, but the gene order or orientation is different amongst the three species.

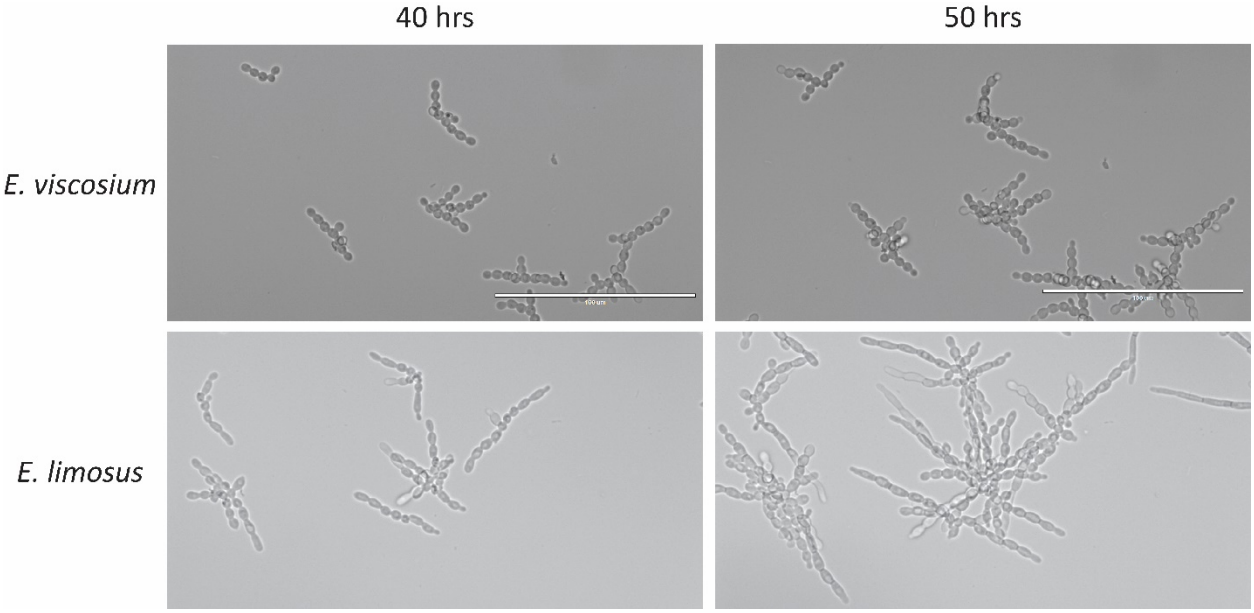

Figure 4: Budding styles of *E. viscosium* and *E. limosus*. Rate of budding is higher is E. limosus than in E. viscosium, as seen at the 50 hrs mark. Budding style is also different between the species, *E. viscosium* buds both distal polarly and proximal at close to a 90° angle, whereas *E. limosus* buds almost exclusively as a distal polar. *E. limosus*'s cells also elongate with every bud, forming almost hyphal-like structures at the 50 hr timepoint.

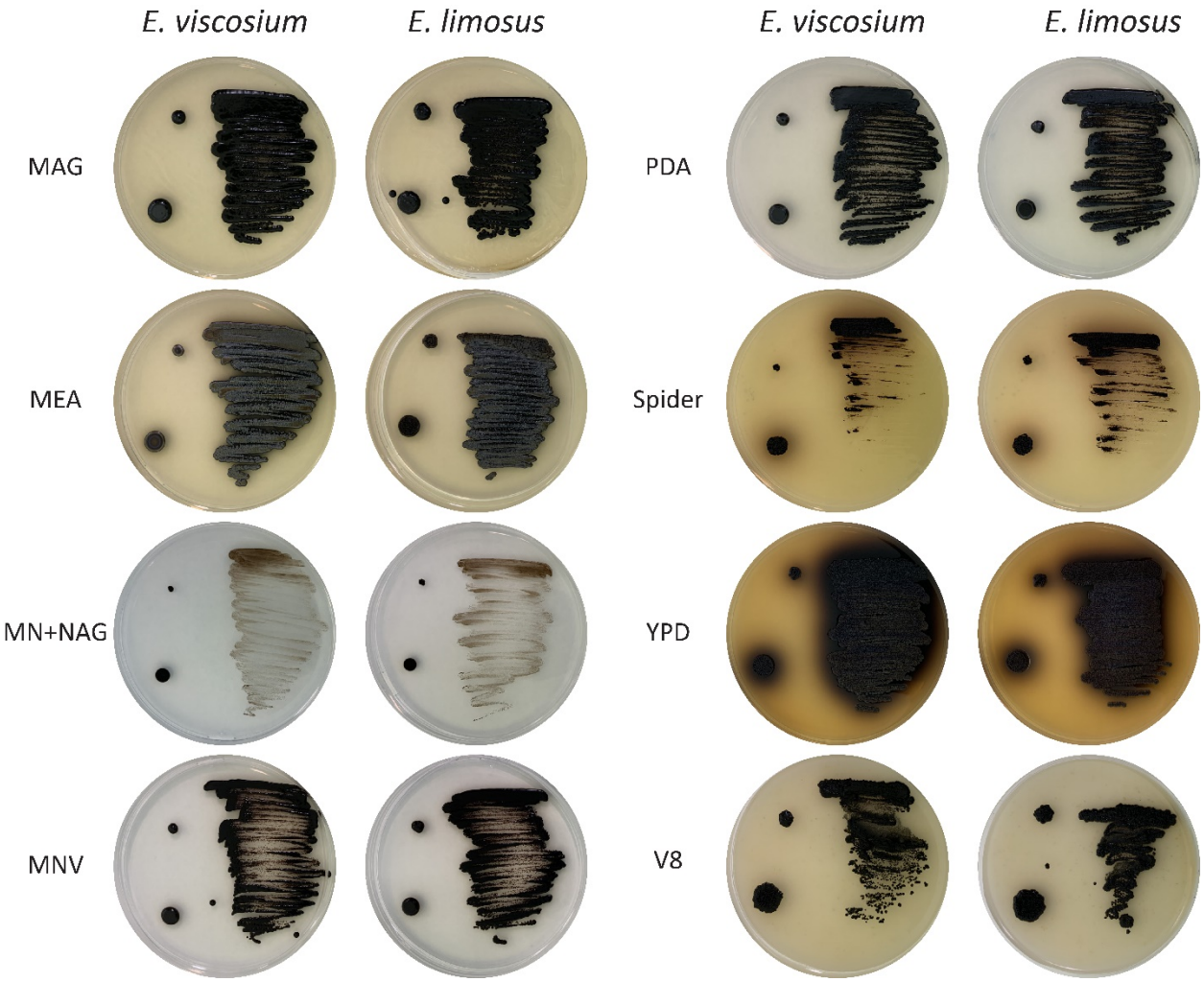

Figure 5: Growth of *E. viscosium* and *E. limosus* on eight different media types. Both species were capable of growth on all medias tested, but growth on MN+NAG showed the least amount of growth. PDA, MAG, and MNV allowed for very shiny and dark colonies to form in both species. Growth on V8 medium confirms potential for saprotrophic growth. Colorful secretions were observed on both Spider media and YPD for both species, though *E. viscosium* has more secretion into YPD than *E. limosus*.

Table 5: Carbon source utilization scores of *E. viscosium* and *E. limosus*

E. viscosium	D-galactose	D-sorbitol	Actidione (cycloheximide)	D-xylose	D-saccharose (sucrose)	D-ribose	N-acetyl-glucosamine	Glycerol	Lactic acid	L-rhamnose	L-arabinose	palatinose	D-cellobiose	Erythritol	D-rafinose	D-melibiose	D-maltose	sodium glucuronate	D-trehalose	D-melezitose	potassium 2-ketogluconate	potassium gluconate	methyl-aD-glucopyranoside	levulinic acid (leuvulinate)	D-mannitol	D-glucose	D-lactose	L-sorbose	Inositol	glucosamine	no substrate	Esculin ferric citrate
1	4	4	5	4	1	2	4	4	3	4	4	3	4	2	1	1	4	2	3	2	4	2	1	4	3	5	1	5	2	1	1	+
2	5	4	4	4	1	2	5	4	3	4	4	3	4	2	1	1	4	2	3	2	3	2	1	3	3	5	1	5	2	1	1	+
3	4	4	4	4	1	2	4	4	3	4	4	3	4	2	1	1	4	2	3	2	4	2	1	4	3	5	1	5	2	1	1	+

Avg	4.3	4.0	4.3	4.0	1.0	2.0	4.3	4.0	3.0	4.0	4.0	3.0	4.0	2.0	1.0	1.0	4.0	2.0	3.0	2.0	3.7	2.0	1.0	3.7	3.0	5.0	1.0	5.0	2.0	1.0	1.0	+
	+	+	+	+	-	V	+	+	V	+	+	V	+	V	-	-	+	V	V	V	+	V	-	+	V	+	-	+	V	-	-	+
E. limosus																																
1	4	5	4	4	2	2	4	4	3	4	4	4	4	1	1	1	4	2	4	2	3	2	1	3	3	5	1	5	2	2	1	+
2	4	5	4	4	2	2	4	4	3	4	4	4	4	2	1	1	4	2	3	2	3	2	1	4	3	5	1	5	2	2	1	+
3	4	5	4	4	2	3	4	4	3	4	4	4	4	2	1	1	4	2	4	2	4	2	1	3	4	5	1	5	2	1	1	+
Avg	4.0	5.0	4.0	4.0	2.0	2.3	4.0	4.0	3.0	4.0	4.0	4.0	4.0	1.7	1.0	1.0	4.0	2.0	3.7	2.0	3.3	2.0	1.0	3.3	3.3	5.0	1.0	5.0	2.0	1.7	1.0	+
	+	+	+	+	V	V	+	+	V	+	+	+	+	V	-	-	+	V	+	V	V	V	-	V	V	+	-	+	V	V	-	+

Figure 6: Growth of (A) *E. viscosium* and (B) *E. limosus* on C32 strips for determining carbon utilization. Both species were capable of using the same carbon sources, though some variations are seen. *E. limosus* was better at growing on palatinose, trehalose, potassium 2-ketogluconate, and mannitol than *E. viscosium*. *E. viscosium* was not better at growing on any carbon sources than *E. limosus*.

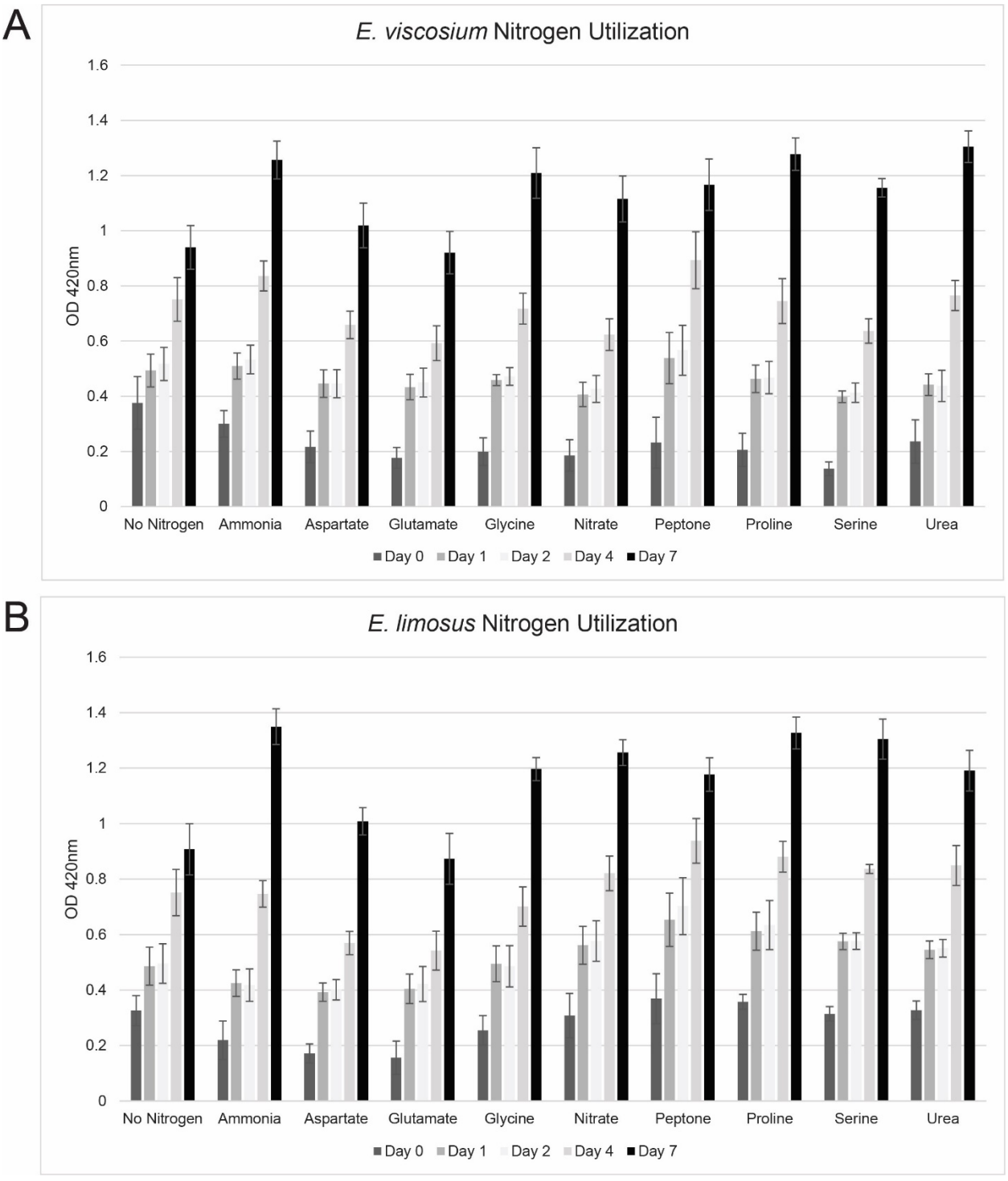

Figure 7: Nitrogen source utilization of *E. viscosium* and *E. limosus* in liquid culture. Neither species was capable of using aspartate or glutamate as a nitrogen source, as their growth amount were equivalent to no nitrogen. All other nitrogen sources tested were used by both species with varying preference. Ammonium was the preferred nitrogen source for *E. limosus*, and *E. viscosium* preferred urea and proline for nitrogen sources.

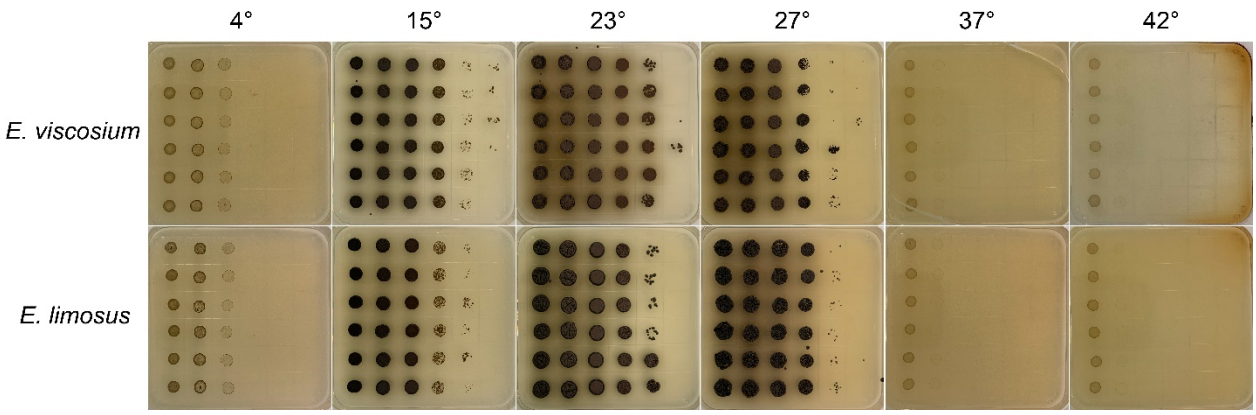

Figure 8: Growth of *E. viscosium* and *E. limosus* at varying temperatures. Neither species was capable of growth at or above 37° C, implying they are not human pathogens. Both species optimally grew at 23° C, but were capable of growth down to 4° C.

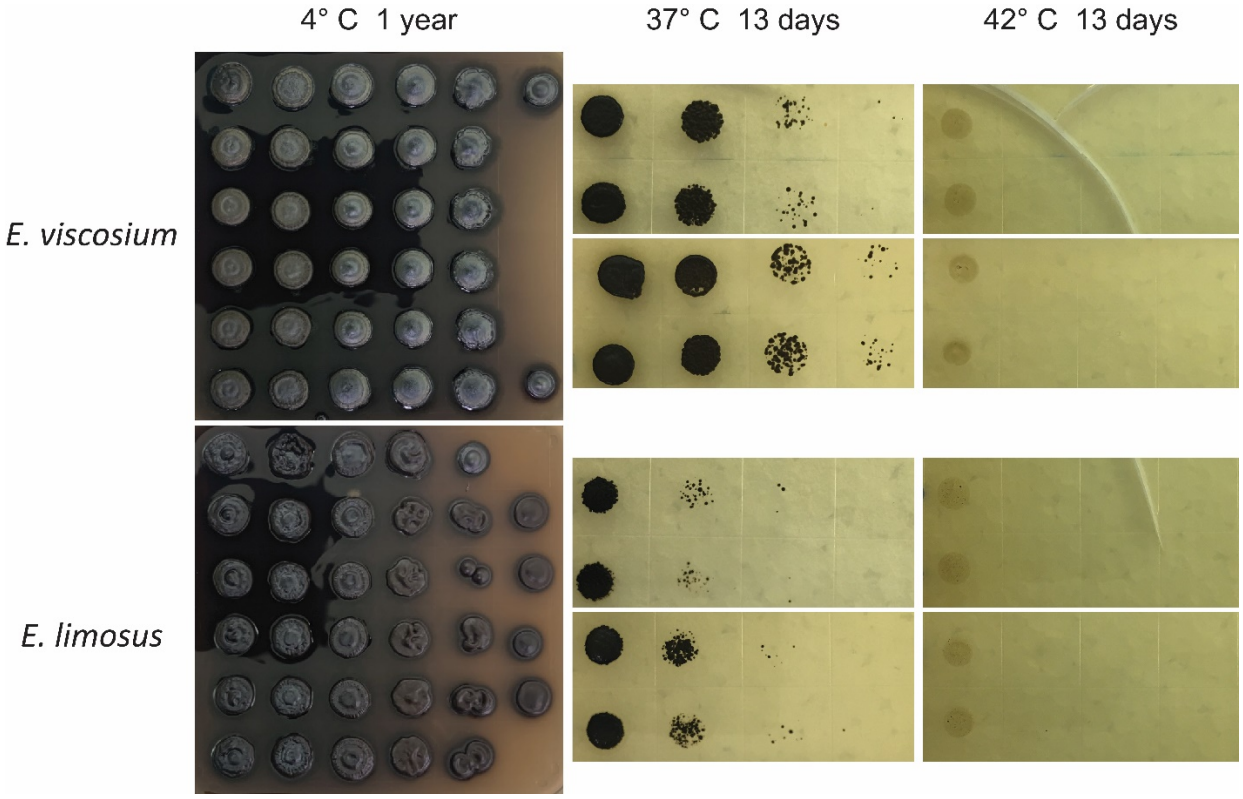

Figure 9: Growth of *E. viscosium* and *E. limosus* at the lowest and highest temperatures tested, after extended periods of time. Growth at 4° C continued for a year in both species, indicating that they can grow at these lower temperatures for extended periods of time. Additionally, we observed that while neither species was capable of active growth at 37° C it also was not too long of an exposure time to kill these cells. Whereas at 42° C neither species was capable of growth and was killed after 48 hrs of exposure.

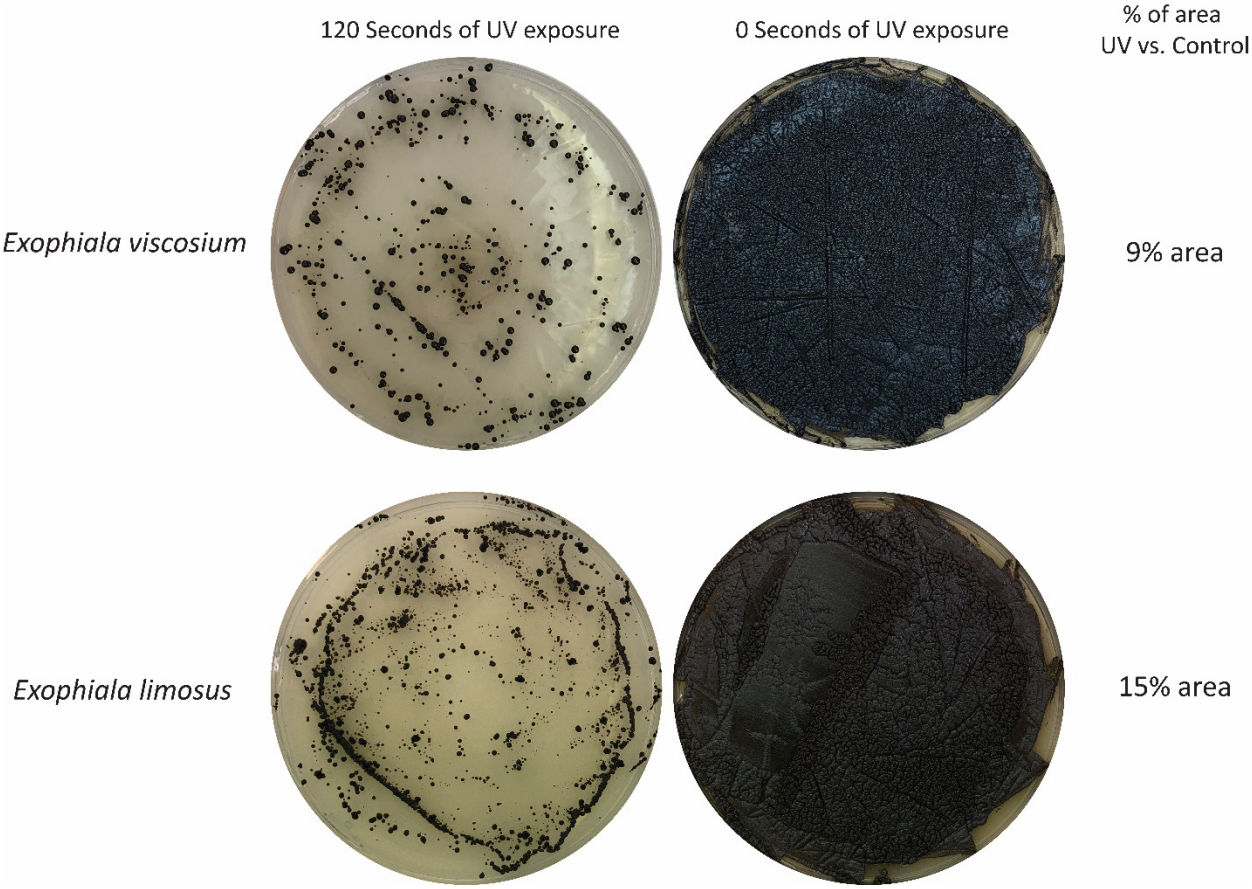

Figure 10: Difference in growth of *E. viscosium* and *E. limosus* with and without exposure to UV light. E. viscosium showed slightly less resistance to the UV exposure than E. limosus. Neither species was mutated from 120 seconds of UV exposure, normally *S. cerevisiae* and *E. dermatitidis* are incapable of growth after the same amount of UV exposure (data not shown).

Table 6: Diameter of the zone of clearing of E. viscosium, *E. limosus*, *E. dermatitidis*, and *S. cerevisiae* with various metals

Species	**$FeSO_4$ 1 M**	**$CoCl_2$ 0.5 M**	**$AgNO_3$ 0.47 M**	**$NiCl_2$ 1.5 M**	**$CuCl_2$ 1.5 M**	**$CdCl_2$ 10 mM**
E. viscosium	1.6 cm	1.5 cm	1.4 cm	3.9 cm	1.3 cm	4.5 cm
E. limosus	1.8 cm	1.8 cm	1.4 cm	4 cm	1.5 cm	3.9 cm
E. dermatitidis	1.3 cm	1 cm	1.5 cm	2 cm	2.5 cm	1.2 cm
S. cerevisiae	1 cm	1.9 cm	2 cm	2.1 cm	2 cm	2.5 cm

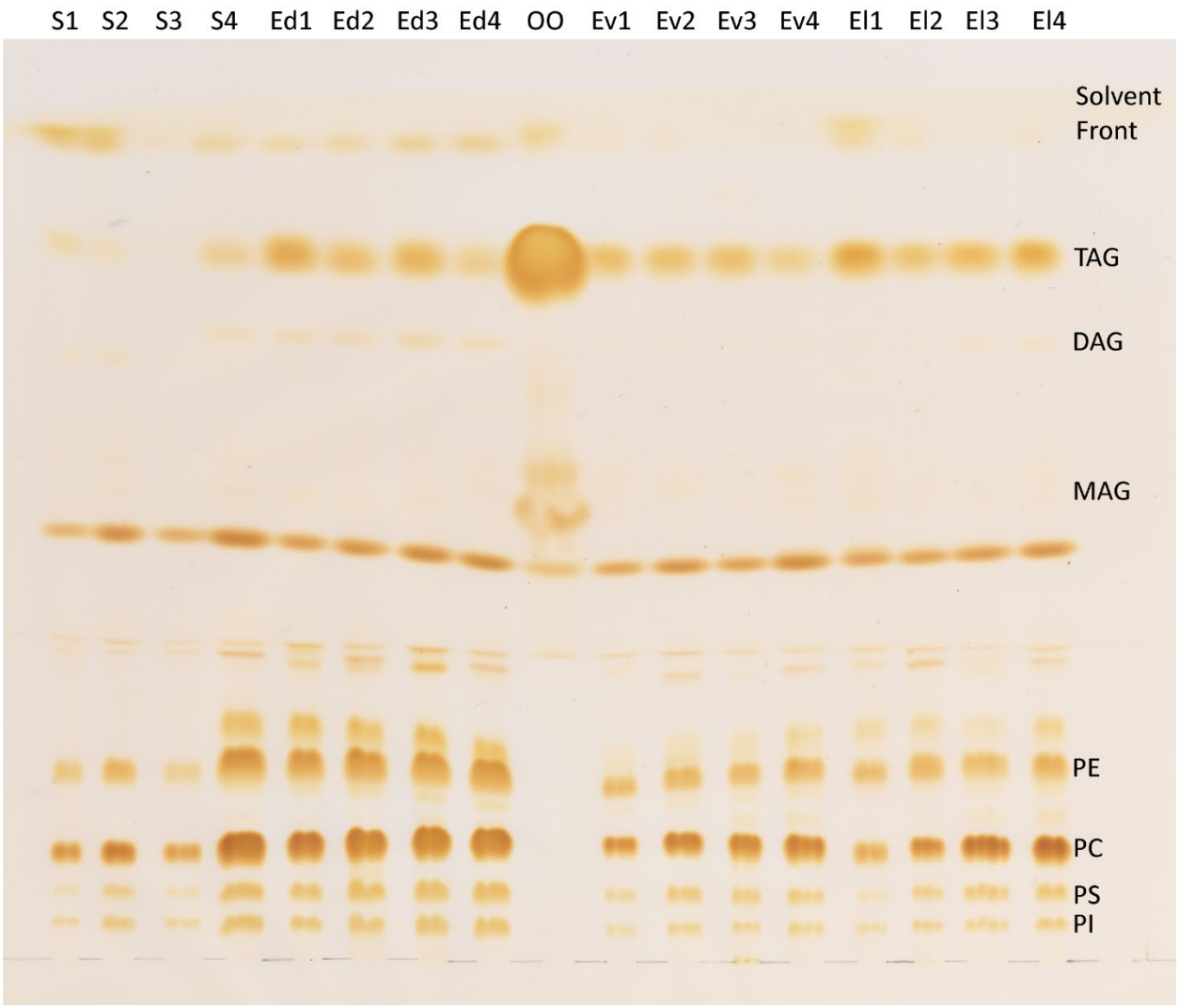

Figure 11: Lipid profile of *S. cerevisiae* (Sc), *E. dermatitidis* (Ed), *E. viscosium* (Ev), and *E. limosus* (El) using four different medias (1: MEA, 2: MEA + % peptone, 3: MEA + glycerol, 4: MEA + glycerol + % peptone). Differences in fermentable vs. non-fermentable carbon sources and amount of nitrogen source did not alter the amount or types of lipids produced by either *E. viscosium or E. limosus*. These fungi also showed no unique lipid production or any extreme accumulations of any lipids when compared to other fungi.

Table 7: Annotation of melanin biosynthetic genes for *E. viscosium* and *E. limosus*.

PKS/DHN/Allomelanin pathway		
Gene in *A. niger*	***E. viscosium* Homolog protein ID #**	***E. limosus* Homolog protein ID #**
Pks1	580617	463165
Ayg1	511449	494160
Arp2	676985	479993, 453709
Arp1	477931	210894
Abr2	603697, 153763	326274, 72468

Abr1	648725, 437535	258543, 441397
	387337, 648725	92776, 258543
	648725, 653857	258543, 102128
DOPA/Eumelanin/Pheomelanin pathway		
Gene in *A. niger*	***E. viscosium* Homolog protein ID #**	***E. limosus* Homolog protein ID #**
MelC2	140179, 643161	84855
	140179	84855
MelO	-	-
McoJ	571417	465594
McoM	571417	465594
McoD	437535	441397
McoG	437535	441397
McoF	437535	441397
McoN	653857, 649741	102128, 454148
McoI	653857, 649741	102128, 454148
L-Tyrosine degradation/Pyomelanin pathway		
Gene in *A. niger*	***E. viscosium* Homolog protein ID #**	***E. limosus* Homolog protein ID #**
Tat	606461	34310
hppD	623446	39306
hmgA	617354, 102643, 403121	430149, 483886, 431641
fahA	617341	148504
maiA	213100	198633

Figure 12

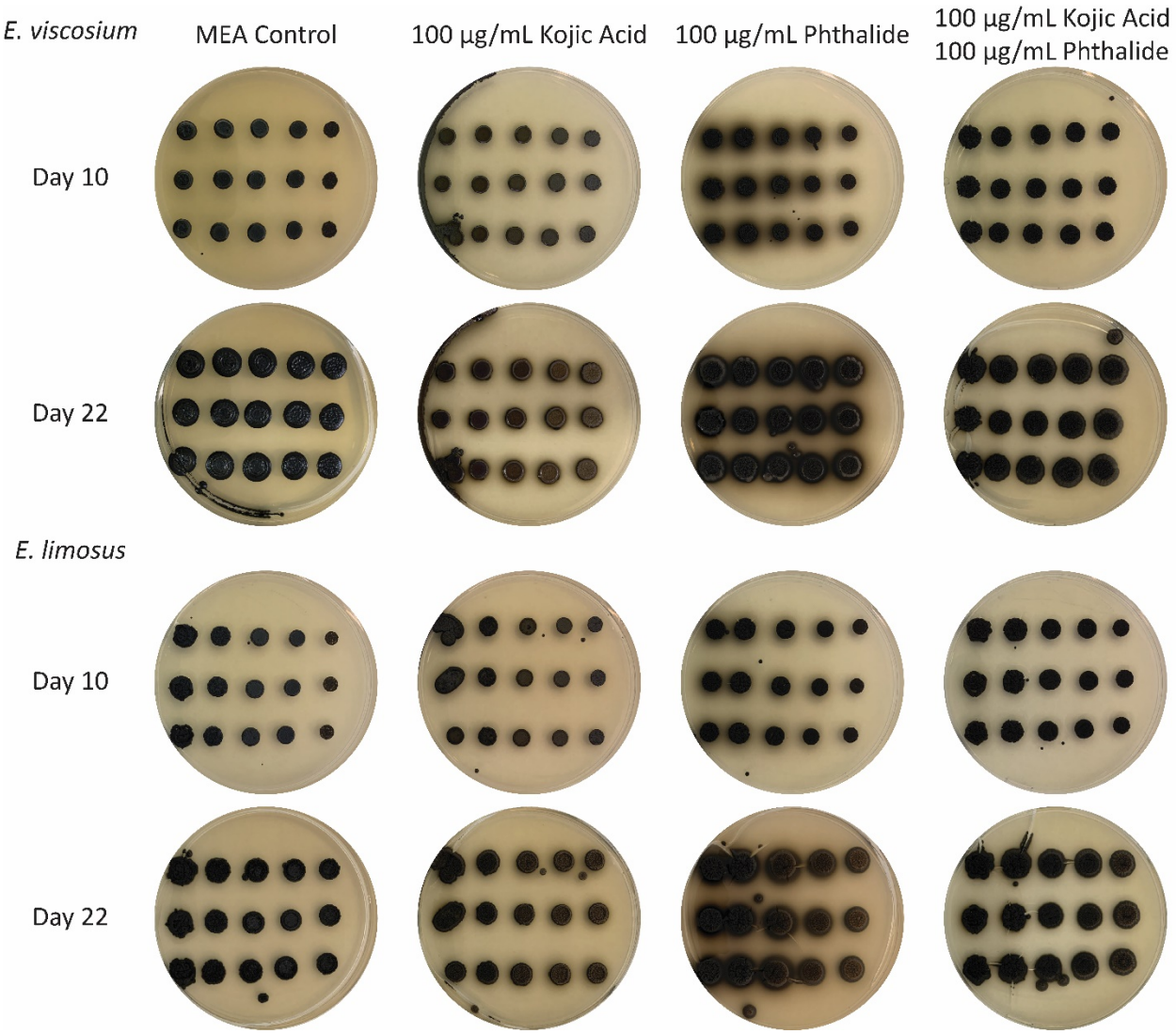

Figure 13: Growth of E. viscosium and E. limosus in the presence of melanin blockers kojic acid and phthalide. Neither chemcial melanin blocker was capable of blocking melanin production in either fungi even when both chemical blockers were used simultaneously. Additionally, use of phthalide on *E. viscosium* induced melanin secretion on a medium where this does not usually occur. The melanin halo around *E. viscosium*'s colonies on medium containing phthalide was replaced with hyphal growth after 22 days.

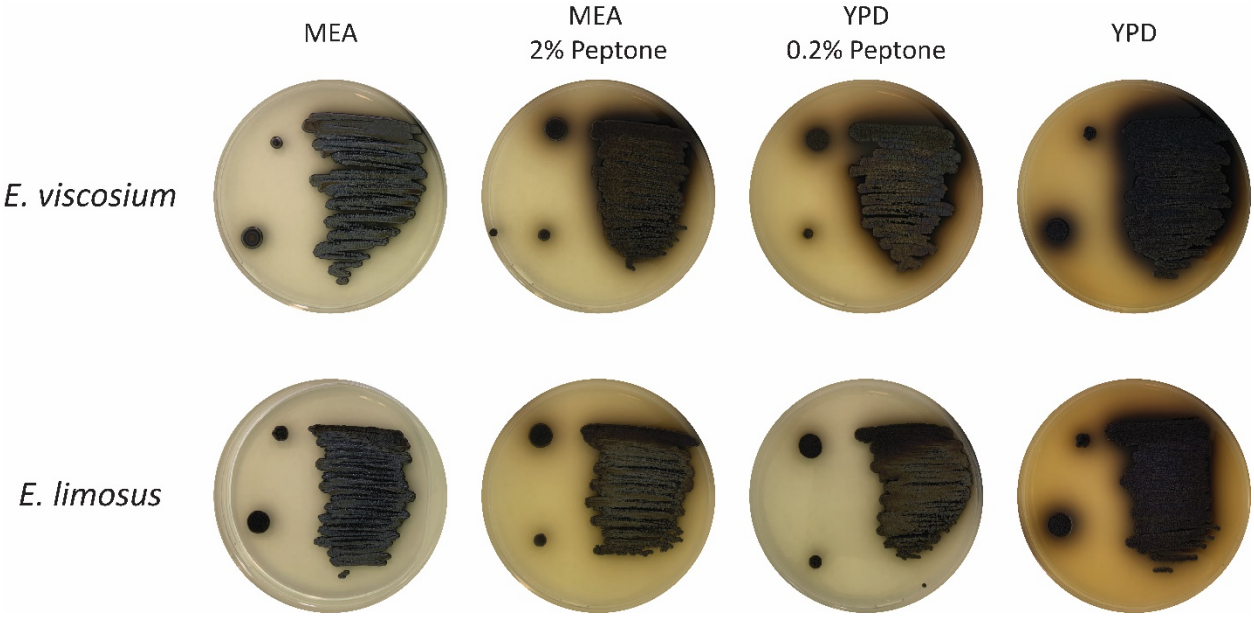

Figure 14: E. viscosium and *E. limosus* grown on MEA and YPD with different concentrations of peptone. *E. viscosium* is capable of melanin secretion on MEA with 2% peptone, which is the same amount of peptone in regular YPD. *E. limosus* was not as capable of secreting melanin in the MEA + 2% peptone, but there is a slight amount of secreted melanin. *E. viscosium* was also capable of secreting melanin on YPD with 0.2% peptone, indicating that yeast extract might have more available nitrogen than malt extract.

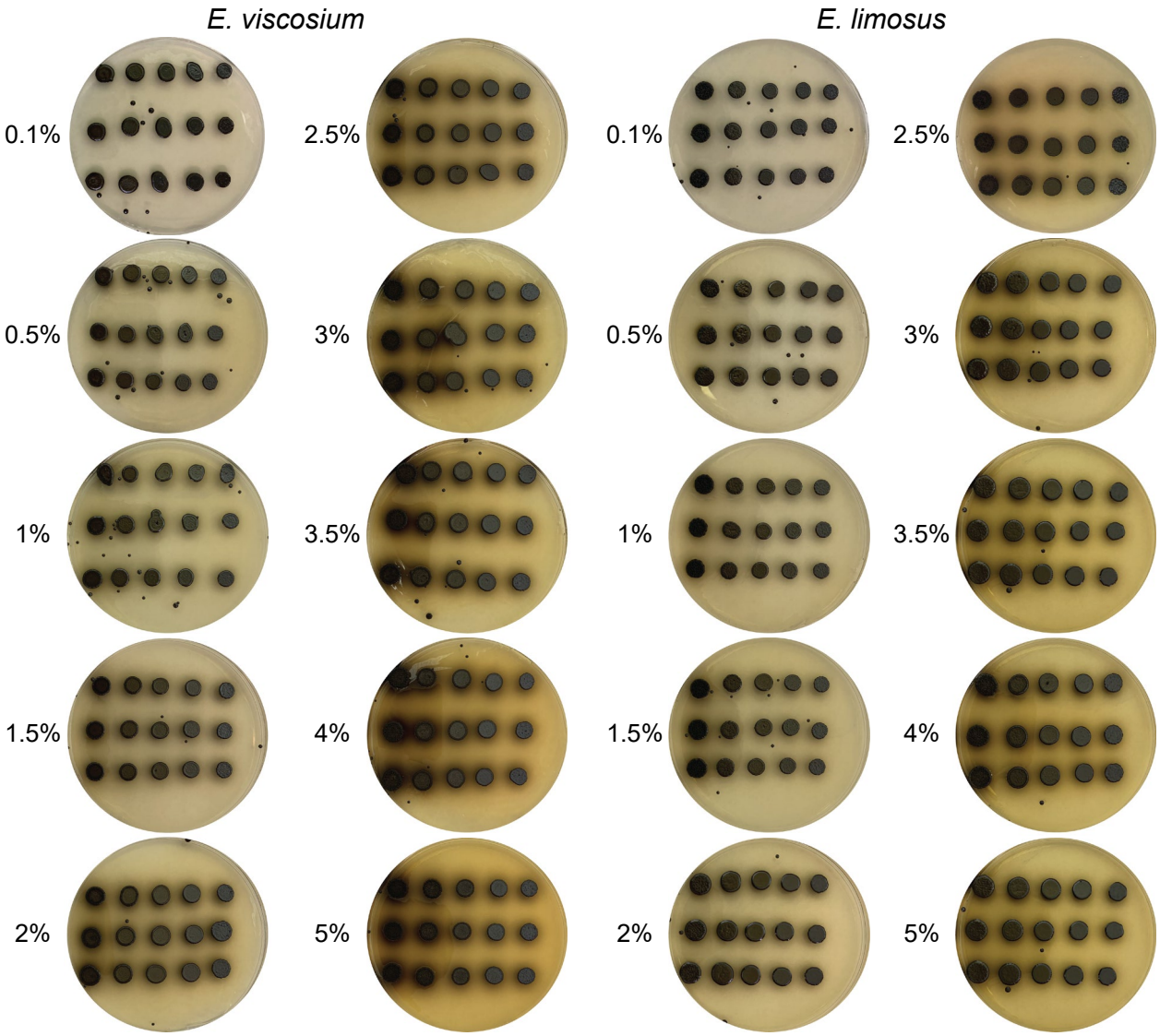

Figure 15: *E. viscosium* and *E. limosus* grown on MEA with increasing amounts of peptone. The higher the amount of peptone in the medium, the more melanin was secreted. *E. viscosium* started secreting melanin at 2%, and *E. limosus* at 4%.

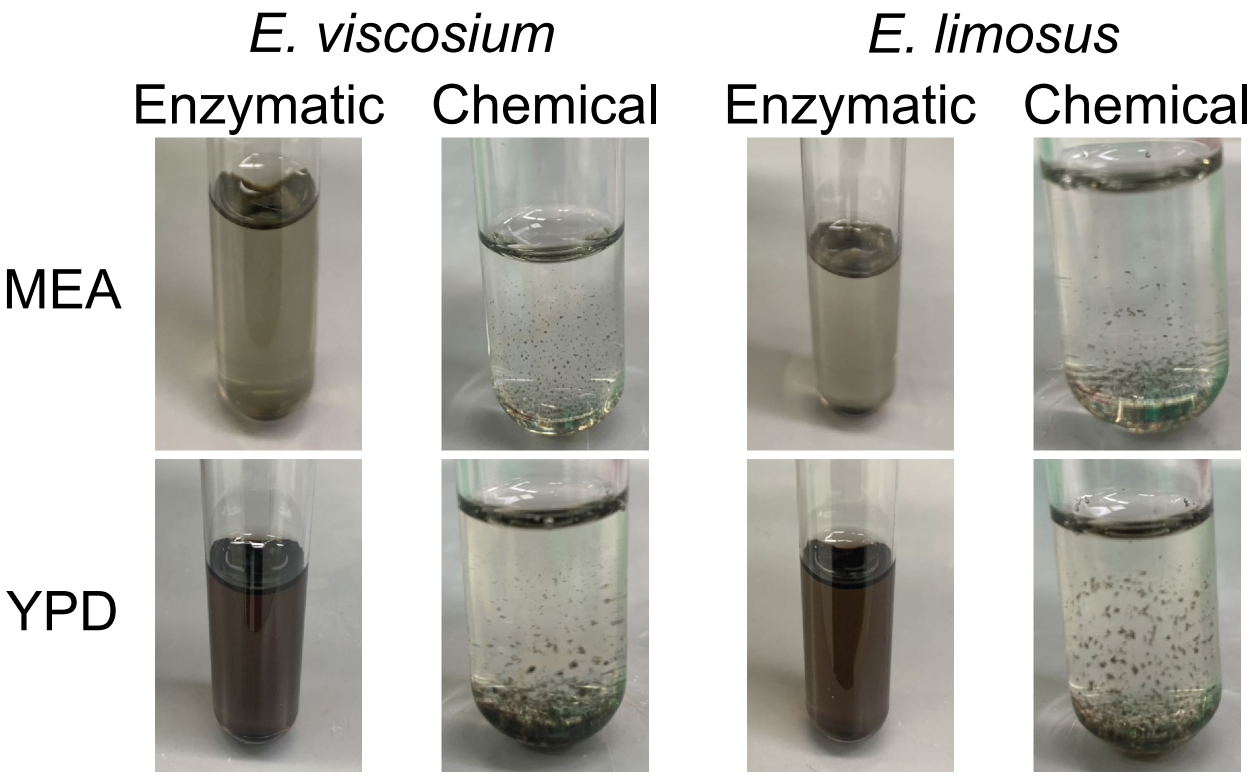

Figure 16: Extraction of melanin from supernatants of *E. viscosium* and *E. limosus* using both enzymatic and chemical methods described in (Pralea et al., 2019). Enzymatic extraction methods were incapable of extracting all the melanin, leaving behind a dark supernatant in the last step. However, melanin extracted by chemical extraction methods had complete extraction of the secreted melanin.

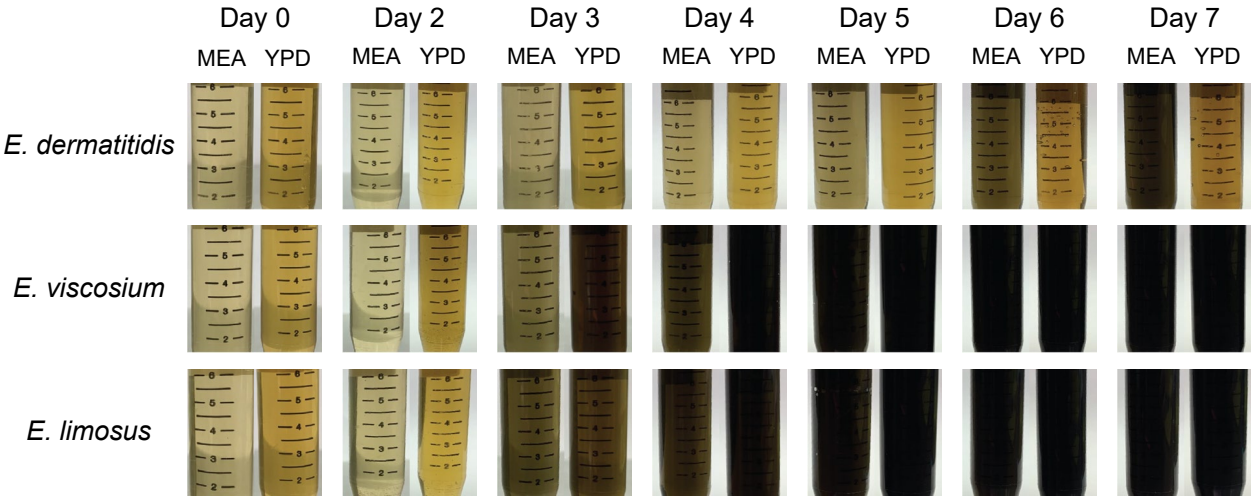

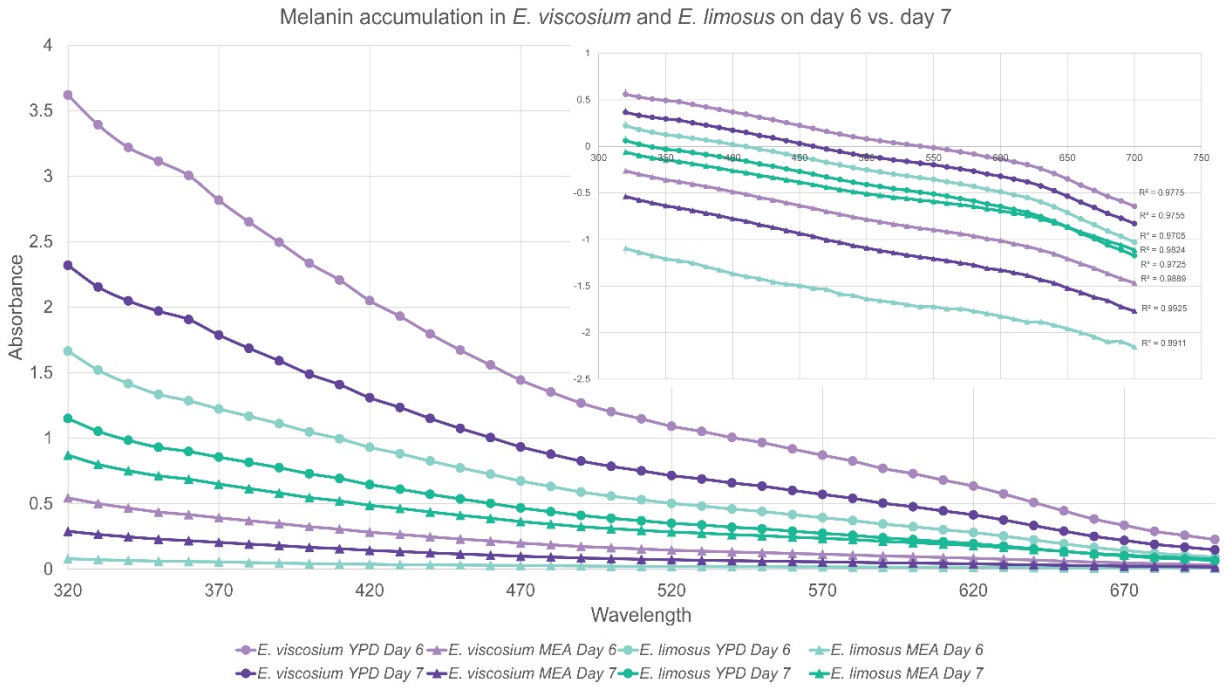

Figure 16: Day 7 results of daily melanin extraction from *E. viscosium*, *E. limosus*, and *E. dermatitidis*. All samples display typical melanin properties with full spectrum light, in that all samples have a linear regression with an R2 value of 0.97 or higher. The sample with the highest amount of secreted melanin on day 7 was *E. viscosium* in YPD. Both *E. viscosium* and *E. limosus* had more secreted melanin when grown on YPD as opposed to MEA which showed lower melanin secretion for both species. *E. dermatitidis* on the other hand had the highest amount of melanin in the supernatant in MEA than on YPD.

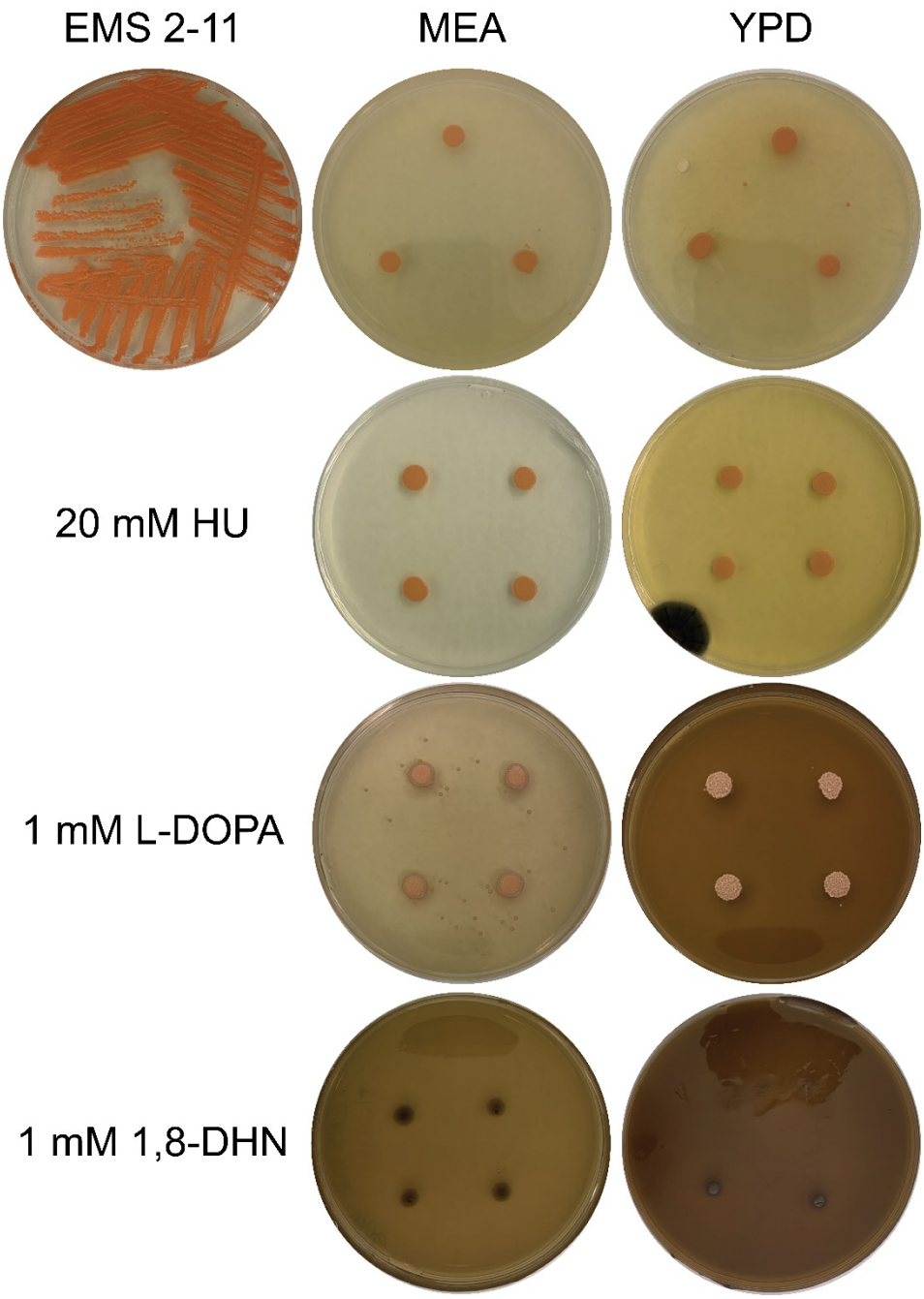

Figure 17: Phenotype of the EMS 2-11 mutant of *E. limosus* with pks1 nonsense mutation, causing melanin production to be stopped hence the pink coloration. Attempts to recover melanin production were done with Hydroxyurea (HU), L-DOPA, and 1,8-DHN. Neither HU or DOPA was able to recover the melanin in the mutant, however 1,8-DHN was able to recover melanin production in this mutant.